



# Imaging Acute Stroke: From One-Size-Fit-All to Biomarkers

Jianfei Lu<sup>1†</sup>, Qiyong Mei<sup>2†</sup>, Xianhua Hou<sup>3†</sup>, Anatol Manaenko<sup>4</sup>, Lili Zhou<sup>5</sup>, David S. Liebeskind<sup>6</sup>, John H. Zhang<sup>7</sup>, Yao Li<sup>8\*</sup> and Qin Hu<sup>1\*</sup>

<sup>1</sup> Central Laboratory, Renji Hospital, Shanghai Jiao Tong University School of Medicine, Shanghai, China, <sup>2</sup> Department of Neurosurgery, Changzheng Hospital, Navy Medical University, Shanghai, China, <sup>3</sup> Department of Neurology, Southwest Hospital, Army Medical University, Chongqing, China, <sup>4</sup> National Health Commission Key Laboratory of Diagnosis and Treatment on Brain Functional Diseases, The First Affiliated Hospital of Chongqing Medical University, Chongqing, China, <sup>5</sup> Department of Neurology, Chinese People's Liberation Army General Hospital, Beijing, China, <sup>6</sup> Neurovascular Imaging Research Core and University of California Los Angeles Stroke Center, University of California, Los Angeles, Los Angeles, CA, United States, <sup>7</sup> Department of Anesthesiology, Loma Linda University School of Medicine, Loma Linda, CA, United States, <sup>8</sup> School of Biomedical Engineering, Shanghai Jiao Tong University, Shanghai, China

## OPEN ACCESS

### Edited by:

Eduardo Candelario-Jalil,  
University of Florida, United States

### Reviewed by:

Saurav Das,  
Washington University in St. Louis,  
United States

Chengcheng Zhu,  
University of Washington,  
United States

### \*Correspondence:

Yao Li  
yaoli118@gmail.com

Qin Hu  
huqinle20010709@126.com

<sup>†</sup>These authors have contributed  
equally to this work

### Specialty section:

This article was submitted to  
Stroke,  
a section of the journal  
Frontiers in Neurology

**Received:** 20 April 2021

**Accepted:** 30 June 2021

**Published:** 23 September 2021

### Citation:

Lu J, Mei Q, Hou X, Manaenko A, Zhou L, Liebeskind DS, Zhang JH, Li Y and Hu Q (2021) Imaging Acute Stroke: From One-Size-Fit-All to Biomarkers. *Front. Neurol.* 12:697779. doi: 10.3389/fneur.2021.697779

In acute stroke management, time window has been rigidly used as a guide for decades and the reperfusion treatment is only available in the first few limited hours. Recently, imaging-based selection of patients has successfully expanded the treatment window out to 16 and even 24 h in the DEFUSE 3 and DAWN trials, respectively. Recent guidelines recommend the use of imaging techniques to guide therapeutic decision-making and expanded eligibility in acute ischemic stroke. A tissue window is proposed to replace the time window and serve as the surrogate marker for potentially salvageable tissue. This article reviews the evolution of time window, addresses the advantage of a tissue window in precision medicine for ischemic stroke, and discusses both the established and emerging techniques of neuroimaging and their roles in defining a tissue window. We also emphasize the metabolic imaging and molecular imaging of brain pathophysiology, and highlight its potential in patient selection and treatment response prediction in ischemic stroke.

**Keywords:** ischemic stroke, tissue window, metabolic imaging, molecular imaging, reperfusion therapy

## INTRODUCTION

Stroke is the worldwide leading cause of death and adult disability. More than 80% of all strokes are caused by brain ischemia, which results from obstruction of one or more cerebral arteries. Rapid and safe restoration of the blood flow through thrombolysis or/and thrombectomy is the only approved therapy for ischemic stroke. Such treatment is strictly limited by a narrow time window and need to be performed within the first few hours after the onset of symptoms (1, 2). The “time is brain” mantra has been the golden principle for acute management of ischemic stroke for decades. Due to the narrow therapeutic window and strict indications, recanalization therapy is restricted to only a small fraction ( $\leq 10\%$ ) of stroke patients<sup>1</sup>. In the past decade, accumulating clinical trials have shown that with the patients selecting by neuroimaging, the time window for reperfusion has been iteratively extended (Table 1) (3–6). The results of these studies revolutionize the field and suggested that “tissue window” might be more personalized than a “time window” to guide precision medicine for ischemic stroke (7, 8). With the rapid development of imaging technology, the ischemic penumbral tissue is now discernible and quantifiable, which provides the possibility to detect salvageable tissue and select the eligible patients for reperfusion therapies (9, 10). A tissue

<sup>1</sup> <https://seekingalpha.com/article/4263610-athersys-stem-cell-therapy-for-ischemic-stroke>

window defined by neuroimaging can serve as surrogate marker for brain physiology in ischemic stroke and facilitate therapeutic decision-making. Here we review the evolution of the time window, address the advantage of tissue window for clinic manage of ischemic stroke, and discuss the roles of neuroimaging in defining a tissue window. We also emphasize metabolic imaging and molecular imaging of brain pathophysiology, and highlight its potential in patient selection and treatment response prediction in ischemic stroke.

## THE EVOLUTION OF TIME WINDOW FOR REPERFUSION THERAPY

The main aim of existing therapies in ischemic stroke is to restore the blood flow quickly and rescue the potentially salvageable brain tissue. After ischemic stroke, the injured brain is characterized by two major zones: the penumbra and the infarct core. The penumbra is the region around the core that neuronal function is partially preserved (11). The fate of penumbral cells critically relies on regional cerebral blood flow (CBF) and it worsens into infarct core in a time-dependent manner. If reperfusion is established during the early hours, cells in penumbra are salvageable (12). On the contrary, the blood flow in the infarct core declines below to 15–20% of the baseline, this would cause irreversibly damage within the first few minutes

of the stroke onset (13). Unfortunately, methods of ischemic core imaging, which is currently in clinical use, are unable to discriminate between incomplete infarction and pan-necrosis. In order to overcome it and revise the clinically relevant parameters more accurately, Goyal et al. suggested replacing the “infarct core” with “ischemic tissue with severity of uncertain viability (SIT-uv)” (14). SIT-uv is considered as tissue that is potentially salvageable by timely reperfusion. Therefore, “time is brain” is still the most important principle guiding reperfusion therapy since the 1990’s (15).

Two primary reperfusion strategies have been demonstrated effectiveness: intravenous thrombolysis with tissue plasminogen activator (tPA) and endovascular thrombectomy with stent retrievers (16). However, the benefits of both tPA and endovascular thrombectomy are strongly time-dependent and restricted to only a fraction of stroke patients due to the narrow time window and strict indications (17, 18). In 1995, tPA was originally recommended to treat ischemic stroke within 3 h of the onset (19). Until 2008, Hacke et al. suggested that administration of tPA could be extended to 4.5 h with computed tomographic scan to exclude the patients with hemorrhage or major infarction (20). Because of the narrow time window and strict contraindications, only 2–5% of patients present with ischemic stroke received tPA (21). Recently, guided by perfusion imaging, the window for thrombolysis with alteplase was extended up to 9 h after onset of stroke (EXTEND trial) (22, 23).

**TABLE 1** | Imaging modalities used in the key clinical trials to expand the therapeutic window of ischemic stroke.

Study	Sample size	Time window	Imaging modalities	Treatment	Implications
EPITHET	101	3–6 h after onset	PWI/ DWI	Alteplase or placebo	Alteplase increased Reperfusion and neurological outcome at 90 days
ECASS III	821	3–4.5 h after onset	CT or MRI	Alteplase or placebo	Alteplase improved neurological outcome at 90 days
MR CLEAN	500	6 h after onset	CTA or MRA	Intraarterial treatment or standard care alone	Intraarterial treatment improved neurological outcome at day 90
EXTEND-IA	70	6 h after onset	CTP	Alteplase with thrombectomy or alteplase alone	Thrombectomy improved reperfusion, early neurologic recovery, and functional outcome
SWIFT PRIME	833	6 h after onset	CTP, or PWI/DWI	tPA, or tPA with endovascular thrombectomy	Thrombectomy showed more effective recanalization than tPA alone
REVASCAT	206	8 h after onset	CT, DWI	Thrombectomy or standard care alone	Thrombectomy reduced the severity of disability
ESCAPE	316	12 h after onset	CT, CTA	Thrombectomy plus standard care or standard care alone	Endovascular thrombectomy benefited the patients with moderate-to-severe ischemic stroke.
DEFUSE-3	182	6–16 h after onset	CTP, PWI/DWI	Thrombectomy plus standard care or standard care alone	Thrombectomy resulted in better functional outcomes than standard medical therapy alone
DOWN	206	6–24 h after onset	DWI, CTP	Thrombectomy plus standard care or standard care alone	Thrombectomy improved the outcomes at 90 days
WAKE UP	503	4.5 h to unknown time of onset	DWI, FLAIR	Alteplase or placebo	Alteplase improved functional outcome at 90 days

CT, computed tomography; CTP, computed tomography perfusion; CTA, computed tomography angiography; MRI, magnetic resonance imaging; MRA, magnetic resonance angiography; DWI, diffusion-weighted imaging; PWI, perfusion-weighted imaging; FLAIR, fluid-attenuated inversion recovery; tPA, tissue plasminogen activator.

However, the authors had certain doubts that positive results of the WAKE-up trail nullified the equipoise and terminated the trail early for this reason (3). Furthermore, due to the small number of patients (225 patients from 27 hospitals over 8 years) and because 80% of the patients had large vessel occlusions, the conclusion of EXTEND trail was not reflected in the current guidelines of American Heart Association (AHA). Still AHA recommended taking into account the conclusion of WAKE-UP trail, which stated that patients, who awoke with stroke or had an unclear time of onset which might be more than 4.5 h of the past (>4.5 h from the last known well) could be treated with IV alteplase (24). The eligibility is magnetic resonance imaging (MRI) mismatch between abnormal signal on diffusion-weighted magnetic resonance imaging (DW-MR) and no visible signal change on FLAIR. Present guidelines also endorsed the usage of tenecteplase in patients eligible to mechanical thrombectomy who do not have contraindications for IV fibrinolysis. There is emerging evidence for the non-inferiority of tenecteplase compared to alteplase, although it has not been widely accepted in clinical practice yet (25).

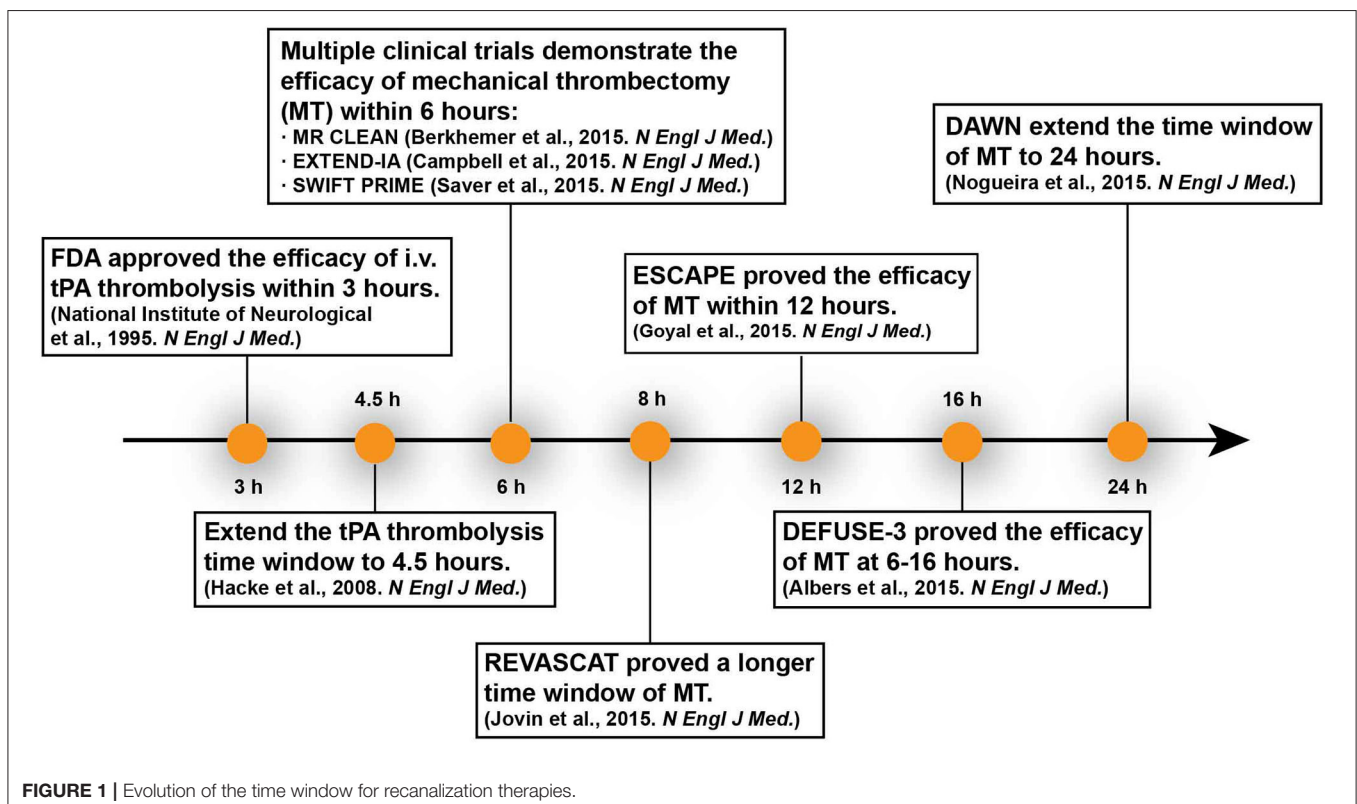
In 2015, it was proven that mechanic thrombectomy with/without intravenous thrombolysis can improve functional outcomes within 6 h after stroke onset (26–28). In patients who have proximal arterial occlusion and small infarct core, mechanical thrombectomy can extend the therapeutic window to 8 h (REVASCAT Trial) even to 12 h (ESCAPE Trial) (29–31). Based on two other recent trials DEFUSE 3 and DAWN, the therapeutic time window can be extended to 24 h since

stroke onset (5, 6). Case studies even reported that delayed thrombectomy days or weeks after onset achieved good clinical outcome (32, 33). Recent animal studies proved that delayed recanalization at 3, 7, or 14 days after permanent middle cerebral artery occlusion (MCAO) led to better functional and histological recovery (34). These researches represent a new milestone in acute stroke therapy (Figure 1). Imaging-based patient selection plays a crucial role in the success of these clinical trials and inspires us to rethink the principle “time is brain.”

The salvageability of the affected brain tissue depends primarily on both the duration and the severity of ischemia. The onset-to-treatment time is not the inflexible determinant of reperfusion therapy when takes the collateral flow into accounts. The more extensive the collateral flow, the longer the brain tissue is tolerant to ischemia. However, the collateral flow is highly variable among individuals, which results in variation in tissue susceptibility and therapeutic window. The current “one-size-fit-all” therapeutic time window does not consider the collateral circulation and varied tissue susceptibility, and how to evaluate the viability of the ischemic tissue quickly and accurately is a challenge for the individualized reperfusion therapy.

## DETECTION OF THE PENUMBRA

The penumbra was first experimentally delineated by Astrup in a baboon MCAO model in 1977. Using somatosensory-evoked potentials, he defined the penumbra as an area surrounding the ischemic core in which neurons are affected but have the



potential for recovery. Neurons in this area are characterized by low electric activity but sustained energy metabolism, and they do not have noticeable morphological damage (35). Because of the invasive method, it was difficult to translate this experimental concept to clinic and improve stroke diagnosis and treatment. Modern imaging techniques such as positron emission tomography (PET), MRI, and computerized tomography (CT) can distinguish salvageable tissue invasively by measuring hemodynamics and energy metabolism. PET is considered as the “gold standard” for penumbra imaging, however, MRI is more favorable in practice. In addition, CT perfusion is being increasingly used for its low cost and wide availability. The strengths and weaknesses of these imaging modalities on penumbra identification are summarized in **Table 2**.

## PET

The existence of penumbra in stroke patients was demonstrated for the first time by PET. In 1981, Baron et al. observed decreased CBF and increased oxygen extraction fraction (OEF) in an ischemic stroke patient by PET and coined this modality as “misery perfusion” which indicated potential viable tissue (36). This area with increased OEF was the original definition of penumbra. Labeling arterial blood sample with  $^{15}\text{O}$  allows PET to assess the regional CBF, OEF and cerebral metabolic rate of oxygen ( $\text{CMRO}_2$ ) ( $\text{CMRO}_2 = \text{CBF} \times \text{OEF} \times \text{arterial oxygen content}$ ) and determine the penumbra. Early PET studies classified the ischemic tissue into 3 regions depending on CBF rate: the infarct core with  $\text{CBF} < 12 \text{ ml}/100 \text{ g}\cdot\text{min}$ , the penumbra with  $\text{CBF}$  of  $12\text{--}22 \text{ ml}/100 \text{ g}\cdot\text{min}$  and the oligemia with  $\text{CBF} > 22 \text{ ml}/100 \text{ g}\cdot\text{min}$  (37–40). In practical applications, the extent of penumbra is dynamic and time dependent process, which

varies with the severity and duration of ischemia. CBF value only reflects the reperfusion status at the time of imaging. An initial severe ischemia may show a normal appearing CBF value because of partial restoration of blood flow, but the ischemic tissue has already irreversibly damaged (37, 41). The advanced  $^{15}\text{O}\text{-O}_2$  PET can detect OEF and distinguish viable tissue from core infarction. Thus, the mismatch between CBF and oxygen metabolism is usually considered as the *in vivo* hallmark of penumbra region, which maintains transient oxygen supply while suffering severe hypoperfusion (40, 42). Recently, some advanced approaches have been used to identify the penumbra.  $^{11}\text{C}$ -flumazenil ( $^{11}\text{C}$  FMZ), a marker of cortical neuron integrity, combine with  $^{15}\text{O}\text{-H}_2\text{O}$  PET can detect early neuronal death irrespective of time elapse and without arterial blood sampling. Based on the specific metabolic parameters, it is well-accepted that PET is the gold standard for determining the penumbra (43, 44).

However, detection of penumbra by PET has several limitations, such as technical difficulty, invasive procedures, exposure to radioactivity and high cost, which prevent PET from broad acceptance in clinical routine (44). Therefore, both improvement of current methods and the development of other imaging modalities are needed.

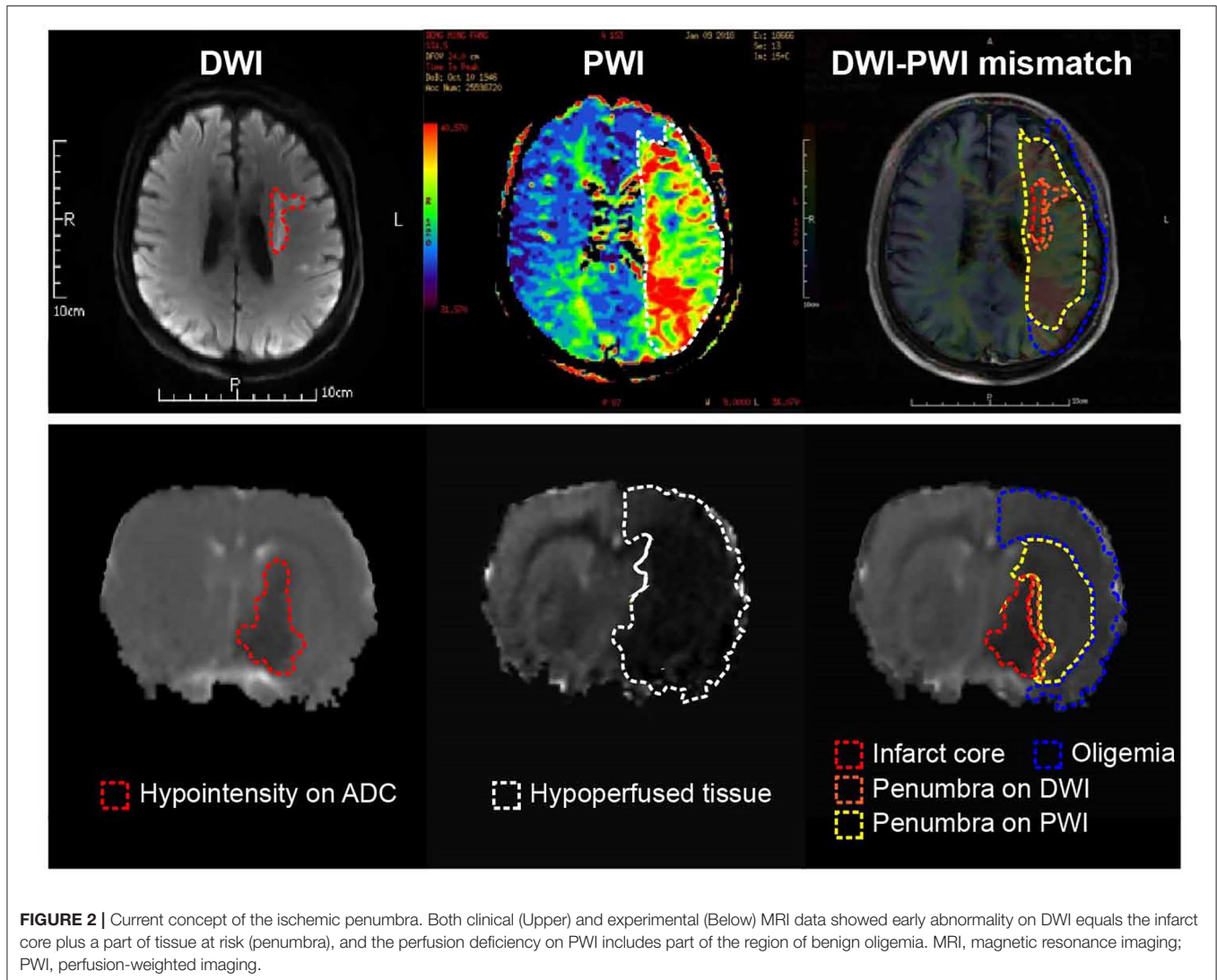
## MRI

Compare to PET, MRI has better spatial and temporal resolution, and no risk of radiation exposure of patients. MRI has largely replaced PET in acute stroke imaging in clinic (45). The MRI-based perfusion-diffusion mismatch (PDM) is a surrogate of PET-based penumbra evaluation (**Figure 2**). Diffusion weighted imaging (DWI) refers to the visualization of random Brownian movement of water molecules in brain tissue. Lower diffusion coefficients generally resulted from energy failure and subsequent cytotoxic edema, and it is suggested to delineate infarct core tissue that irreversibly damaged (**Figure 3**) (46). Perfusion weighted imaging (PWI) measures brain perfusion dynamically with such parameters as CBF, cerebral blood volume (CBV), mean transit time (MTT) and time to peak (TTP) (**Figure 3**) (47). PWI abnormality provides the information on both infarct core and the surrounding hypoperfused tissue. Volumetric-based PDM is usually defined as a mismatch ratio of  $\text{PWI}/\text{DWI} \geq 1.2$ , which is postulated to represent the penumbra that locates outside the infarct core but is at risk of infarction (48). The concept of PDM has been proved practically in both experimental and clinical studies (49–51). Early clinic studies have shown that salvage of brain tissue delineated by the PDM improved neurological functions (52, 53), and selection of patients with PDM increased the rate of reperfusion and achieved favorable clinical response when treated within 6 h (54, 55). However, this surrogate marker of penumbra is challenged by several limitations (44). Comparative PET/MRI studies confirmed the mismatch area imprecisely depicts elevated OEF and overestimated the penumbra from benign oligemia defined by PET. Because of the wide variation in thresholds, DWI also overestimates the infarct core by including part of the penumbra (56–58). And as the viability and metabolic state of brain tissue strongly depends on the duration of ischemia, for those “wake-up” patients who didn’t know stroke onset time

**TABLE 2** | Comparison of strengths and weaknesses of different imaging modalities for penumbra identification.

	Parameters	Strengths	Weaknesses
PET	$^{15}\text{O}$ -OEF $^{15}\text{O}$ -rCBF $^{15}\text{O}$ - $\text{CMRO}_2$	Gold standard	Technical difficulty Invasive procedure Radiation High cost
MRI	DWI/PWI $^{23}\text{Na}/^1\text{H}$ MRI Sodium MRI DWI/SWI T2* OC/PWI	Easy-to-use Good spatial resolution High sensitivity Non-invasive No radiation	Time-consuming High cost Inaccuracy
CT	CBF CBV MTT TTP Tmax	Widely accessible Easy-to-use	Radiation Contrast agent required Hard to standardization

PET, positron emission tomography; MRI, magnetic resonance imaging; CT, computed tomography; OEF, oxygen extraction fraction; rCBF, regional cerebral blood flow;  $\text{CMRO}_2$ , cerebral metabolic rate of oxygen; DWI, diffusion weighted imaging; PWI, perfusion weighted imaging; SWI, susceptibility-weighted imaging; OC, oxygen challenge; CBF, cerebral blood flow; CBV, cerebral blood volume; MTT, mean transit time; TTP, time to peak; Tmax, time to maximum.



(SOT), it is hard to set threshold of the parameters [such as TTP and time to maximum (Tmax)] (57).

Accumulating evidence has shown that there was no clear association between PDM and penumbra (59–62), and the inaccuracy of PDM in defining penumbra may be responsible for the failure of some reperfusion and neuroprotection therapies in clinic (63, 64). It is urgent to develop novel imaging paradigms that can serve as a clinical marker of penumbra. Several attempts have been made to improve the accuracy of PDM in penumbra predicting. Combined  $^{23}\text{Na}$ -MRI to  $^1\text{H}$ -MRI was developed to complement PDM and serve as a viability marker for penumbra detection in several animal models. Tissue sodium concentration increased in the core and decreased in the penumbra so that the viable penumbra could be differentiated from the core in transient MCAO rats (65, 66). In addition, it has been proposed that sodium MRI may help determine the SOT by calculating this retrospectively (67, 68). Susceptibility-weighted imaging (SWI) is also used to identify the penumbra in stroke patients. SWI detects the paramagnetic

susceptibility difference between deoxygenated and oxygenated hemoglobin, which reflects the OEF of brain tissue (69). DWI-SWI mismatch is shown to be a promising marker for evaluating penumbra (70). In addition, by mapping the ratio changes of deoxyhemoglobin/oxyhemoglobin,  $T_2^*$  oxygen challenge combined PWI assessed the viability of penumbra serially and showed advantages over PDM for penumbra detection (71).

### Computed Tomography Perfusion (CTP)

CTP is an imaging technique that is increasingly used for determination of infarct core and penumbra in acute ischemic stroke patients. The clear advantages of this technique are its easily accessibility and fast acquisition (72). Similar to PWI MRI, raw data of CTP is also displayed in parameter maps, including CBF, CBV, MMT, TTP, and Tmax. Regions with dramatically reduced CBF or CBV correspond to the core infarction, while regions with prolonged MTT, TTP, or Tmax delineate the penumbra (Figure 4) (73). However, there is significant

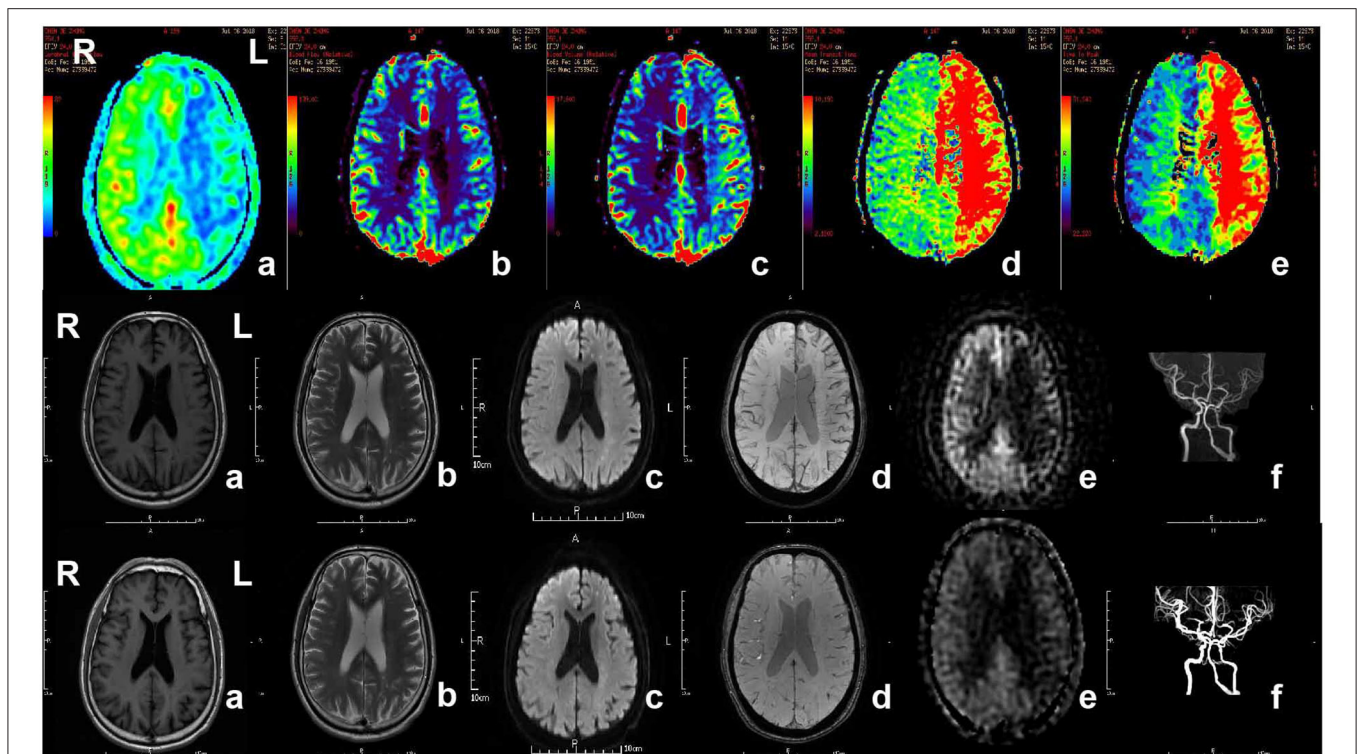


**FIGURE 3 |** MR imaging of the patient with acute ischemic stroke. The patient, 71-year-old male, suffered from weakness of right limbs, alalia and was unable to walk 3 h prior to the imaging. Medical history included hypertension, diabetes and varicosity of both lower extremities. Physical examination showed right facial paralysis, the muscle strength of right limbs was grade I, right Babinski sign (+), Chaddock sign (+), and NIHSS score was 13. The diagnosis of the patient is acute ischemic stroke. The patient was given multimodal MRI and MRA before and after recanalization. The first row showed perfusion-weighted imaging. a and b, Lower CBF in left cerebral hemisphere. c, Higher CBV in left cerebral hemisphere. d, Longer MTT in left cerebral hemisphere. e, Longer TTP in left cerebral hemisphere. The second row and third row showed MRI and MRA before recanalization and after recanalization, respectively. a, b, and c, In the left frontal lobe and lateral ventricle had sporadic dots with slightly longer T1 signal, longer T2 signal higher signal, respectively, in T1WI, T2WI, DWI. d, No cerebral microbleeds in SWI. e, Original ASL. f, MRA showed the intracranial segment of the left internal carotid artery and the left middle cerebral artery were significantly narrow in the second row, while recanalization got in left internal carotid artery and middle cerebral artery. MR, magnetic resonance; MRA, magnetic resonance angiography; SWI, susceptibility weighted imaging; ASL, arterial spin labeling; CBV, cerebral blood volume; CBF, cerebral blood flow; TTP, time to peak; MTT, mean transit time.

variability in CTP technique between different CT scanners, processing software and prior institutional optimization, and this results in controversy about the accurate measurement of penumbra (74). Moreover, due to the delay of the arrival of contrast to brain, CBV calculation always results in an overestimation of the core lesion that leads to an underestimation of penumbra (75). CTP still has the risk of radiation exposure and toxicity of the contrast agent.

## METABOLIC IMAGING OF ISCHMEIC STROKE

For patients excluded from reperfusion therapy due to exit of the therapeutic time window established by imaging strategy mentioned above, there is another opportunity to expand the treatable population: selecting of the patients by advanced physiologic imaging. Both MRI-based PDM and CTP depend on selecting threshold values of blood flow to differentiate the penumbra from infarct core and benign oligemic brain tissue. And these thresholds change with the evolution of stroke. So

far, there are no validated thresholds that accepted for routine penumbra imaging in the clinical setting. Parameters which display the physiology of brain immediately and independently of the onset-time are in urgent need to delineate penumbra accurately and guide the precision therapy in stroke. When the blood flow is compromised, energy metabolism disturbance occurs within seconds as brain has very limited supply of energy producing substances and relies on oxidative metabolism to meet its tremendous energy requirements (76, 77). The metabolic stress induces ionic perturbations and oxidative stress which trigger the cascade of pathophysiological events ultimately resulting in neuronal death (78). Accumulating evidence has suggested that energy status is associated with cell survival and determines the fate of ischemic tissue (79–81). Direct measurement of the metabolic status provides more accurate information to delineate the viable tissue. Therefore, energy metabolism can serve as a direct indicator of the salvageable tissue in the penumbra zone. Quantification of cerebral oxygen metabolism has shown great promise in revealing the viability of ischemic tissue during stroke. Several imaging modalities, such

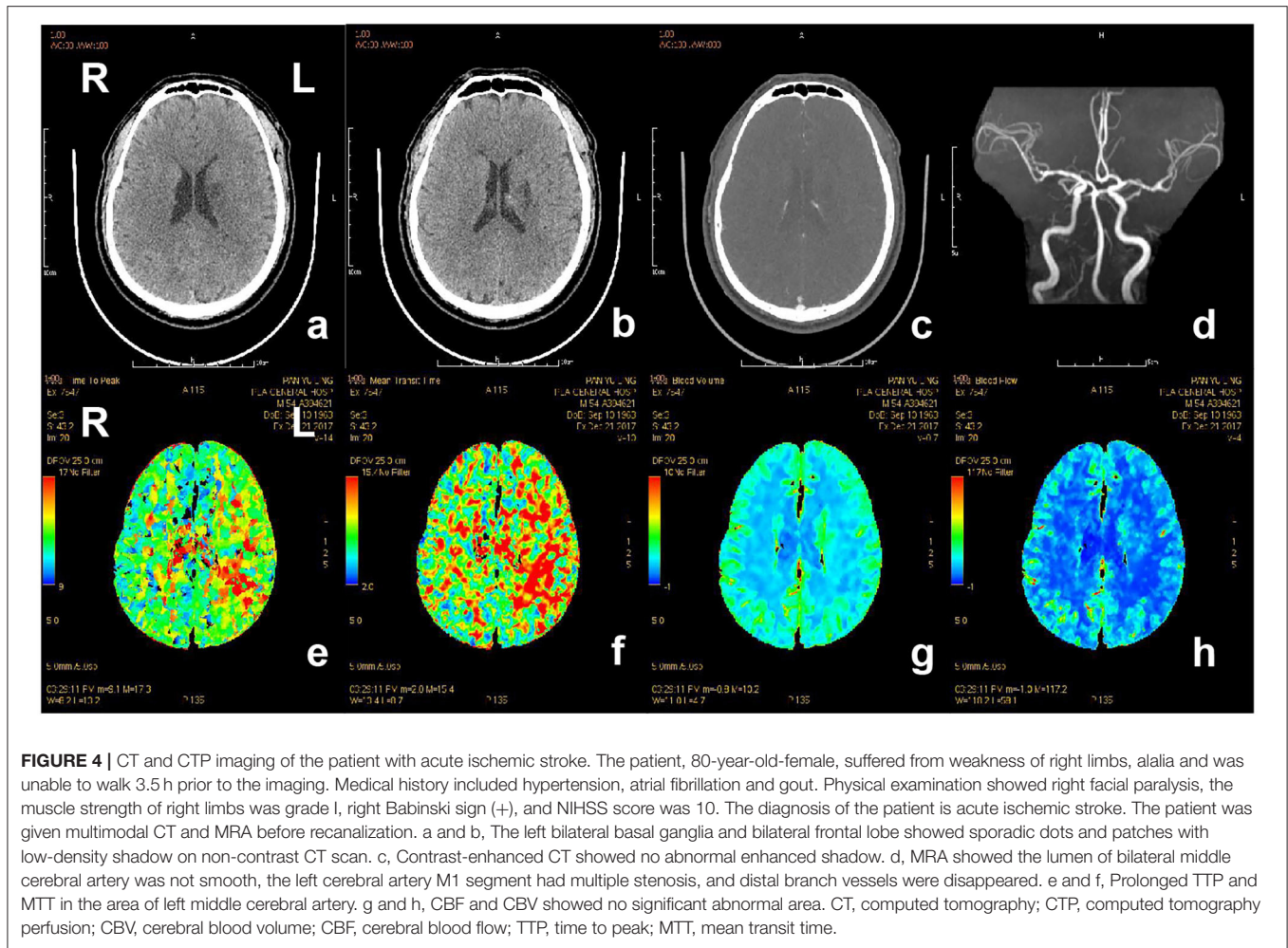


**FIGURE 4 |** CT and CTP imaging of the patient with acute ischemic stroke. The patient, 80-year-old-female, suffered from weakness of right limbs, alalia and was unable to walk 3.5 h prior to the imaging. Medical history included hypertension, atrial fibrillation and gout. Physical examination showed right facial paralysis, the muscle strength of right limbs was grade I, right Babinski sign (+), and NIHSS score was 10. The diagnosis of the patient is acute ischemic stroke. The patient was given multimodal CT and MRA before recanalization. a and b, The left bilateral basal ganglia and bilateral frontal lobe showed sporadic dots and patches with low-density shadow on non-contrast CT scan. c, Contrast-enhanced CT showed no abnormal enhanced shadow. d, MRA showed the lumen of bilateral middle cerebral artery was not smooth, the left cerebral artery M1 segment had multiple stenosis, and distal branch vessels were disappeared. e and f, Prolonged TTP and MTT in the area of left middle cerebral artery. g and h, CBF and CBV showed no significant abnormal area. CT, computed tomography; CTP, computed tomography perfusion; CBV, cerebral blood volume; CBF, cerebral blood flow; TTP, time to peak; MTT, mean transit time.

as PET and MRI, have been applied to image cerebral oxygen metabolism in both experimental research as well as clinical practice (82). These imaging methods and parameters they can detect are summarized in **Table 3**. Furthermore, we review the most recently advances in metabolic imaging, which may greatly facilitate routine clinical applications to guide optimal therapy decision for acute ischemic stroke as well as subacute or chronic stroke with permanent large vessel occlusion.

### PET Metabolic Imaging

As mentioned above,  $^{15}\text{O}$  multi-tracer PET can provide the tomographic distributed imaging of brain oxygen extraction and metabolism. More importantly, it is the reference standard for quantitative evaluations of OEF,  $\text{CMRO}_2$ , CBV, and CBF. In the late 1970's, scientists successfully measured the regional brain CBV and CBF, and oxygen metabolism in stroke patients with  $^{15}\text{O}$ -labeled PET, and distinguished the severely hypoperfused but potentially salvageable tissue from the irreversibly damaged (83–85). Using  $^{15}\text{O}$ - $\text{H}_2\text{O}$  PET, Heiss et al. found that the misery perfused tissue was salvaged by early intravenous thrombolysis (86). This study is a millstone in stroke research. It revolutionized the management of acute stroke patients by demonstrating the

positive result of rt-PA. However, due to the technical complexity,  $^{15}\text{O}$  PET is not widely performed in clinical settings, with issues involving requirement of on-site cyclotron and radiochemistry facility because of the short half-life of  $^{15}\text{O}$  (2 min), real-time artery blood sampling and analyzing to obtain the regional CBF (rCBF), as well as complex post processing (87). Efforts have been made to streamline the  $^{15}\text{O}$ -PET examination for routine clinical practice, including: (i) quantitative voxel-by-voxel maps of rCBF without a direct arterial input function (88); (ii) shortening the clinical examination period by dual-tracer ( $\text{H}_2^{15}\text{O}$  and  $^{15}\text{O}_2$ ) autoradiography approach (89); and (iii) developing non-invasive techniques to assess CBF, OEF, and  $\text{CMRO}_2$  (90). Attempts were also made in animal stroke studies. Methodological inventions, such as intravenous administration of injectable  $^{15}\text{O}_2$  and inhalation of  $^{15}\text{O}_2$  gas, had been tried to facilitate the evaluation of  $\text{CMRO}_2$  and OEF in small animals (91–93). These developments potentiate the possibility of using PET in clinical routine to expand the treatable stroke patients in early stage.

The improvement of the radiotracers has revolutionized the use of PET in measuring OEF and  $\text{CMRO}_2$  and mapping the cerebrovascular reserve and the penumbra. The newly

**TABLE 3** | The three major imaging methods for acute stroke and physiological parameters they can detect.

	Parameters	PET	MRI	CT	
Metabolism	Oxygen metabolism	<sup>15</sup> O-OEF <sup>15</sup> O-CMRO <sub>2</sub>	OCI		
	Neuronal death	<sup>11</sup> C-FMZ			
	Hypoxia	<sup>18</sup> F-FMISO Cu-ATSM			
	pH		APT-MRI <sup>13</sup> P MRS		
	Lactate		<sup>1</sup> H MRS <sup>13</sup> C MRS		
	NAA		<sup>1</sup> H MRS		
	PCr/Pi		<sup>13</sup> P MRS		
	ATP		<sup>13</sup> P MRS		
	Pathophysiology	Excitotoxicity		<sup>1</sup> H MRS GluCEST	
		Apoptosis		<sup>1</sup> H MRS	
Inflammation		Cu-ATSM TSPO	SPIO/USPIO		
			MNP-PBP MPIO		
BBB leakage			DCE-MRI	DCE-CT Micro-CT	

FMZ, flumazenil; MISO, misonidazole; Cu-ATSM, Copper-based Radiopharmaceuticals; APT, amide proton transfer; MRS, MR spectroscopy; NAA, N-acetylaspartate; PCr, phosphocreatine; Pi, inorganic phosphate; ATP, adenosine triphosphate; CEST, chemical exchange saturation transfer; SPIO/USPIO, small and ultrasmall superparamagnetic iron oxide particles; MNP-PBP, magnetic nanoparticle-P-selectin binding peptide; MPIO, microparticles of iron-oxide; TSPO, translocator protein; DCE, dynamic contrast-enhanced.

developed PET ligands, including radio-labeled FMZ, radio-labeled fluoromisonidazole (FMISO), and copper-based radiopharmaceuticals (Cu-ATSM) have been explored to delineate the disease in preclinical and clinical research. In 1997, <sup>11</sup>C-FMZ PET was used to indicate the development of infarction in cat stroke model and showed the potential to select eligible patients for early therapeutic intervention (94). In 2000, a clinical trial proved that <sup>11</sup>C-FMZ PET was able to differentiate the viable tissue from the irreversibly damaged at the early stage of acute stroke (95). In this study, the areas with reduced perfusion but preserved <sup>11</sup>C-FMZ binding could benefit from reperfusion therapy, while the areas with <sup>11</sup>C-FMZ uptake defects were permanent lesions. Thiel et al. reported that <sup>11</sup>C-FMZ PET could be used to estimate rCBF in ischemia without arterial input function (96). However, the application of <sup>11</sup>C-FMZ PET in clinical practice is limited by several issues: the requirement of cyclotron to produce <sup>11</sup>C, the regional expression of benzodiazepine receptors in cerebral cortex, and the low affinity of <sup>11</sup>C-FMZ to bind with its receptor at the acute phase of ischemia/reperfusion (97). New PET tracers are still in urgent need to meet the clinical requirements.

Compared with <sup>11</sup>C-FMZ PET, <sup>18</sup>F-FMISO PET is more broadly used (98). In a preclinical study, <sup>18</sup>F-FMISO microPET was used to map the brain hypoxia in the acute stage of

permanent distal MCAO rats, and supported that <sup>18</sup>F-FMISO might be a marker of core area as well as of penumbra (99). Besides, <sup>18</sup>F-FMISO uptake was also used to predict the tissue fate. The patients without <sup>18</sup>F-FMISO uptake had no infarct growth on the follow-up DWI, while those with abnormally increased <sup>18</sup>F-FMISO uptake showed grown infarct (100). And white matter was reported to take up more <sup>18</sup>F-FMISO than gray matter, indicating stronger resistance to ischemia than gray matter (101). However, the penumbra outlined with <sup>18</sup>F-FMISO may be overestimated. When using <sup>18</sup>F-FMISO in ischemic stroke patients, large regions of hypoxic tissue was found surrounding the ischemic core, which spontaneously reverted back to normal (102). The major drawback of <sup>18</sup>F-FMISO PET is the slow kinetics of <sup>18</sup>F-FMISO, which requires 2–3 h to clear it from the hypoxic tissue. A faster kinetic and metabolic rate tracer is needed for metabolic imaging. Compared with nitroimidazole, Cu-ATSM is rapidly washed out, and the imaging can be finished with 20–30 min after injection (103). Cu-ATSM has also been proved to modulate inflammation and has therapeutic potential in experimental stroke (104).

## MRI Metabolic Imaging

Studies have investigated MR-based PWI and DWI, and suggested the PWI-DWI mismatch regions as potentially salvageable tissue (51). This clinical routine protocol does not define metabolic activity directly; however, PWI and DWI clearly indicate different metabolic regions. The following sections will carefully discuss related major MRI metabolic imaging techniques, which have been summarized in Table 2.

## Magnetic Resonance Spectroscopy

MRS acquires the signal arising from brain metabolites by analyzing molecules such as hydrogen ions or protons. Because of high spatial and temporal resolution, proton MRS (<sup>1</sup>H MRS) is the more commonly used. The most assessed metabolites with potential value for clinical stroke evaluation are lactate (1.30 ppm) and tNAA (2.02 ppm) (105–107). Preclinical studies have shown that levels of total N-acetylaspartate (tNAA) decrease to 50% in the first 6 h after ischemic stroke, followed by a milder decrease to 20% for the subsequent 24 h, and gradually returned to 30% until 7 day (107). Clinically, the concentration of tNAA in penumbra and in core infarction may even decrease below the level of detection (108, 109). Severely decreased tNAA is related to serious clinical syndrome and extensive infarction, which means poor clinical outcome (110). Lactate is the end product of anaerobic glycolysis and rises within minutes after ischemic stroke. Elevated lactate in the core of ischemic tissue is positively related to the final infarct size and neurological deficits (111). The increase of lactate accompanied with reduction of tNAA was observed in patients with large infarction and poor outcome (110). Therefore, the level of lactate and tNAA is important for evaluating the severity of stroke and predicting the recurrence of ischemic events (112). Interestingly, a recent MRS stroke animal study suggested that ML3 (bis-allylic protons of polyunsaturated fatty acids, 2.80 ppm), which was detected of a significant increase at 7 days after stroke, may be a non-invasive surrogate biomarker

of cumulative apoptosis in stroke, which could be used as a clinical predictive marker (107).

$^{13}\text{P}$  MRS is also used to evaluate brain energy metabolism in ischemic stroke by assessing the high energy phosphate metabolism, particularly adenosine triphosphate (ATP) and creatine phosphate (PCr) (113). A gradual decrease in ATP was only exhibited in severe stroke, not mild stroke (114). The ratio of PCr to inorganic phosphate (Pi) (PCr/Pi) showed a precipitous decrease during ischemia as well as reperfusion (114). Cerebral intracellular pH can also be measured by  $^{13}\text{P}$  MRS. It was calculated by the chemical shift ( $\delta$ ) of the Pi resonance peak relative to the PCr resonance peak (115).

Though MRS is of great value in assessing the severity of ischemia and predicting the risk for recurrence, low signal-noise ratio, long sequence duration and the risk of lipid contamination make MRS not suitable for routine assessment of acute ischemic stroke patients.

### Oxygen Challenge Imaging

Oxygen challenge imaging (OCI) is based on blood oxygen level-dependent (BOLD) contrast MRI that reflects the changes in blood oxygen saturation. OCI uses transient hyperoxia during  $T_2^*$ -weighted MRI to present dynamic changes in deoxyhemoglobin concentration. Therefore, tissues in the penumbra exhibit an increase in  $T_2^*$  signal intensity, with diminished or absent  $T_2^*$  signal intensity in the infarct core. Time to peak value from OCI offers additional information to facilitate the identification of at-risk tissue in ischemic stroke rats (116). The region of OCI response was reported to be larger than the PWI-DWI mismatch region (117). The  $T_2^*$  OCI was developed using 100% normobaric hyperoxia and has showed clinical translational potential for stroke diagnosis. However, inhaled 100% oxygen induces sinus artifacts in the front lobe. Decreasing the concentration of inhaled oxygen can decrease these artifacts, but makes more difficult to distinguish the penumbra from surrounding tissues (117). Recently, the combination of 40% oxygen and perfluorocarbons and fluorinated hydrocarbons with respiratory gas significantly enhanced  $T_2^*$  response to 40% oxygen in  $T_2^*$  defined penumbra (118). The same group also developed the GOLD (Glasgow Oxygen Level Dependent) diagnostic imaging method by using  $T_2^*$  oxygen challenge ( $T_2^*\text{OC}$ , 100% inhaled oxygen) combined with lactate change MRS technique (119). This method worked concurrently to identify the salvageable tissue in penumbra based on the glucose metabolic status in MCAO rats. However, the disadvantages of OCI are, as mentioned above, the poor signal-to-noise due to the limited oxygen that delivered to the tissues and the artifacts caused by the paramagnetic effect of 100%  $\text{O}_2$  within the paranasal sinuses (120).

### pH-Weighted Imaging

Zhou et al. developed a new MRI approach which was predominantly sensitive to the intracellular pH changes (121). This method benefited from the chemical exchange processes, which amide protons transfer between cellular peptides and proteins in a pH-dependent manner. Because amide proton transfer (APT) is pH dependent, measures of APT may be used

to measure pH value (122). Acute ischemic stroke causes an accumulation of lactic acid and results in the decrease of pH, which could be the earliest sign for the tissue at risk. Accordingly, there were research data which suggested that pH imaging could be used to define the ischemic penumbra. The hypoperfused tissue with normal ADC and low pH may represent ischemic penumbra (121, 123, 124). A further study suggested that an additional pH-weighted imaging with PWI-DWI was superior to PWI-DWI alone to predict the tissue outcome in ischemic stroke rats (125).

Although most early studies, which investigated pH-weighted imaging technique, were performed in rodents, there is increasing translation of this technique to human studies. Tietze et al., for the first time, demonstrated that clinical application of pH-weighted imaging in acute stroke patients was possible and could be quantified, which carried potential for providing additional information on metabolic changes in acute ischemia (126). Subsequently, scientists from Oxford successfully identified the ischemic penumbra using pH-weighted magnetic resonance imaging (127).

Although studies related to pH-weighted imaging have provided important insights in the pathology of acute stroke, they currently cannot be applied in clinical routine due to their technical limitations, such as hardware constraints of human MRI scanner (short repetition time and strong radio-frequency saturation power), acquisition protocols selection (single-slice or volumetric APT imaging) and analyzing techniques (128). Consequently, pH-weighted imaging studies have paid more attention to develop better quantifying approaches and improve the APT MRI sensitivity to pH, thus, the acidosis in ischemic penumbra can be more reliably delineated (128–130).

### Other Metabolic Imaging Techniques

There are many other imaging modalities that are at early stage of ischemic metabolic imaging, such as sodium imaging, PET  $^{17}\text{O}$  imaging, and MR-derived cerebral metabolic oxygen index (MR COMI) (131). While metabolic imaging is promising, emerging imaging technologies require considerable validation to consider how they fit into the current imaging protocols and what information they accurately provide to guide the recanalization therapy. Many of these techniques will require technical refinement before they can be used in clinical acute ischemic stroke.

## MOLECULAR IMAGING OF PATHOPHYSIOLOGY

Ischemia causes the shortage of glucose and oxygen and subsequently depletion of ATP, which result in the dysfunction of sodium-potassium pump and membrane depolarization (132). That induces multiple pathophysiological cascades, including excitotoxicity, apoptosis, acidosis, blood-brain barrier (BBB) leakage, and immune response, which lead to ischemic neuronal loss (133).

Several imaging techniques have been used in the visualization of ischemic stroke pathophysiology (134). For example, ischemia

results in marked reduction of tissue pH that triggers neuronal death (135). As mentioned above, pH-weighted MRI can detect the changes of tissue pH value that reflect the progress of acidotoxicity. MRS can evaluate tissue levels of lactate and ML3 that on this way estimate the status of acidosis and apoptosis. Current developments of pathophysiology imaging facilitate the *in vivo* assessment of pathophysiological markers and therapeutic targets after stroke, and provide the opportunities for the translation of multimodal imaging strategies in stroke diagnosis and treatment. The pathophysiological parameters that can be detected are summarized in **Table 2**.

## Visualization of Excitotoxicity

Excitotoxicity caused by excessive release of glutamate is one of the major culprits that responsible for the neuronal death and neurological deficits after stroke. The levels of glutamate can be detected by  $^1\text{H}$  MRS. In MCAO model in rats, Ramos-Cabrer et al. demonstrated that the levels of glutamate increase in center of the infarction core and then spread to the peri-infarction. Within 24 h after stroke, glutamate levels decreased significantly in the infarct core area, whereas regular levels were detected in the periphery of the core lesion (136). A clinical research found the differences of glutamate levels between infarct core and reperfused ischemic penumbra. In the ischemic stroke patients who received intravenous tPA within 4.5 h, high glutamate concentrations in peri-infarct were observed in the hyperperfused patients, while glutamate concentrations were low in the non-hyperperfused patients (137). The evaluation of glutamate depends on the magnetic field strengths. At low magnetic field scanner, the peak of glutamate and glutamine are consecutive that cannot distinguish glutamate from glutamine. At field strengths of 3.0 T or higher, the separation of glutamate and glutamine is feasible. Besides,  $^1\text{H}$  MRS technique requires long acquisition times and has low spatial resolution.

Recently, a new MRI technique for imaging glutamate has been developed based on chemical exchange saturation transfer (CEST) effect. The CEST effects of amide and hydroxyl protons have also been used to measure pH value changes after ischemic stroke. It has been demonstrated that middle cerebral artery occlusion (MCAO) induced about 100% elevation of glutamate CEST (GluCEST) in the ischemic tissue compared with the contralateral side in rats. This method images the relative changes of glutamate and has the advantages of high spatial and temporal resolution. However, GluCEST imaging is only achievable in the human brain in ultrahigh field (7.0 T) and is not currently accessible in the clinic (138).

## Monitoring the Neuroinflammation and Immune System

The immune system plays a pivotal role in the response to ischemia and the eventual recovery of function (139). The complex cascade of immune cells and inflammatory factors contribute to the breakdown of BBB. After stroke, microglia immediately respond to the ischemic insult, followed by the proliferation of macrophages, dendritic cells, and lymphocytes. With the occurrence of BBB breakdown, neutrophilic cells permeate the infarct and peri-infarct region. The immune cells

release excessive pro-inflammatory cytokines (i.e., TNF- $\alpha$  and IL-1 $\beta$ ) and produce large amounts of free radicals, which contribute to the upregulation of cell adhesion molecule and further propagate the inflammatory response (133). Additionally, inflammation elevates production of matrix metalloproteinases (MMPs) and myeloperoxidase, both of which are major factors leading to BBB breakdown.

After ischemic stroke, the spatiotemporal profile of neuroinflammation with cellular and molecular MRI has been increasingly explored. In cellular and molecular MRI, paramagnetic contrast agents such as gadolinium chelates and small particles of iron oxide were used to detect specific leukocyte populations or molecular inflammatory markers after stroke. Several pre-clinical and clinical studies have demonstrated the application of contrast agents to image the monocyte infiltration after ischemic stroke. The most common strategy for labeling circulating monocytes is the administration of iron oxide nanoparticles. For the labeling, two kinds of particles can be used: small and ultrasmall superparamagnetic iron oxide particles (SPIO and USPIO, respectively) (140–144). SPIO and USPIO shorten the transverse relaxation times  $T_2$  and  $T_2^*$ , and the cells taken up SPIO or USPIO present hypointense on  $T_2$  or  $T_2^*$ -weighted images. Rausch et al. found that USPIOs distributed in patches within the lesion and surrounding area on the first 2 days. On day 4, USPIOs expanded within the lesion core. On day 7 they were found predominantly within the boundary area. This strategy has been used in some human studies to detect macrophage activity in stroke patients (140, 141). With the target-specific contrast agents, molecular MRI have shown the potential to examine inflammation markers *in vivo* in experimental stroke. Jin et al. designed a magnetic nanoparticle-P-selectin binding peptide (MNP-PBP) to image endothelial P-selectin and E-selectin. MNP-PBP showed a notably greater  $T_2$  effect in the infarction and had a tighter binding affinity with selectin (145, 146). Vascular cell adhesion molecule (VCAM-1) and MMPs are other targets for neuroinflammation imaging. In a pre-clinical study, researchers developed microparticles of iron-oxide (MPIO), an MRI contrast agent that could bind with VCAM-1 on the cerebral vascular endothelium and visualize the expression of VCAM-1 (147). The result showed the spatial extent of VCAM-1 was considerably larger than the lesion core area measured by DWI MRI. The authors thought that this molecular MRI imaging of VCAM-1 might include both ischemic core and potentially salvageable penumbral regions.

Microglial activation can be monitored by PET imaging with related molecular biomarkers. The 18 kDa translocator protein (TSPO) system is the most commonly used target system for neuroinflammatory imaging. Due to the activation of microglia, the TSPO density is elevated after ischemic stroke. Furthermore, it has been demonstrated that using [ $^{11}\text{C}$ ] vinpocetine, a prospective radio ligand of TSPO, the regional changes of TSPO can be measured in the brain of ischemic stroke patients (148). The elevated level of TSPO which indicated the activated microglia was found both in the ischemic core and peri-infarct area.

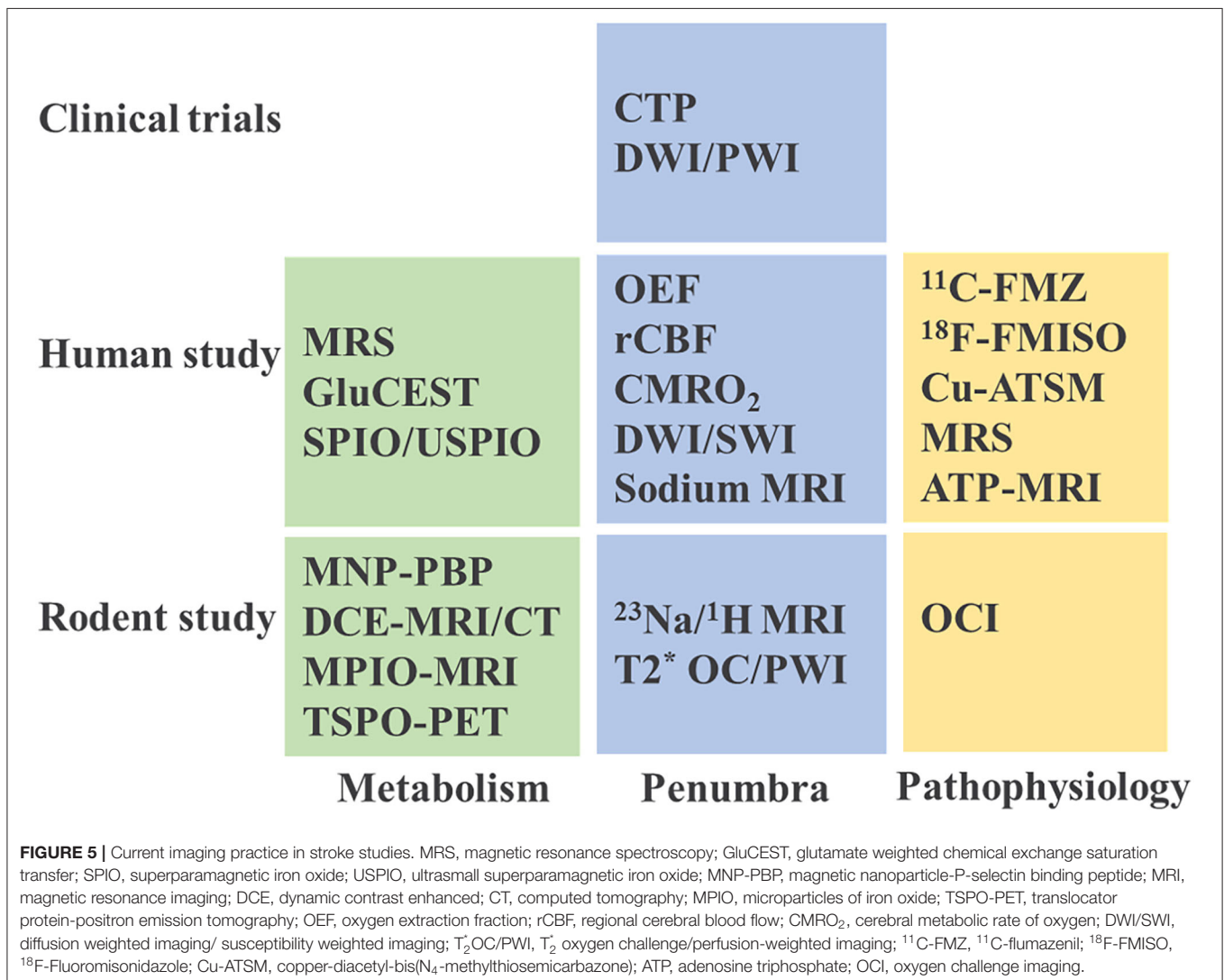
As far as imaging modalities concern there are only a few options, which allow do discriminate different cell types in

the infarcted tissue of patients. Molecular MRI has shown promising futures regarding monitoring of inflammatory cells such as neutrophils, leukocytes and microglia, but it is unable to provide the information in regards of cell viability. Furthermore, the molecular MRI is currently not highly specific and the interpretation of obtained results is sometimes challenging. The toxicity of contrast agents is another concern. All these shortcomings complicate the clinical implementation of this imaging technique.

### Imaging Blood-Brain Barrier Leakage

Restoration of blood flow can induce reperfusion injury, reperfusion injury is one of the events that compromises the BBB. The leakage of BBB, which has been reported have a biphasic pattern, can cause severe brain edema and hemorrhagic transformation (149, 150). MRI and CT are the most widely used clinical imaging tools to evaluate BBB disruption by detecting the extravasation of the intravenously administered small molecular weight contrast agents (151).

Dynamic contrast-enhanced MRI (DCE-MRI) is considered as the gold standard MRI approach to evaluate BBB permeability (152). Gadolinium-diethylenetriamine penta-acetic acid and its variant gadolinium-diethylenetriamine penta-acetic acid-bis (methylamide) are the most used contrast agents that are given as intravenous bolus injection. The accumulation of contrast agents in the extracellular matrix of ischemic tissues results in increased longitudinal relaxation rate and hyperintensity in  $T_1$ -weighted MRI. DCE-MRI exploits this  $T_1$  enhancement to extract quantitative or semi-quantitative information regarding BBB integrity (153). Several pre-clinical studies using DCE-MRI assessed BBB integrity after ischemic stroke. The results consistently have shown a biphasic pattern of BBB permeability after ischemic stroke. Compared to sham-operated animals, the BBB permeability on ipsilateral striatum increased at 4 h after the onset of ischemic stroke. Compared to the 4 h value, a significant decline of stroke-induced BBB disruption was observed at 24 h. Another rise of BBB permeability followed at 48 h. At this time point, the BBB disruption was more prominent than at both 4



and at 24 h after stroke induction (154). The mechanisms of this partial recovery in BBB function are not completely understood. Besides, biphasic pattern of BBB permeability has not been categorically confirmed in stroke patients.

CT can also be used to evaluate BBB integrity. Similar with DCE-MRI, DCE-CT involves intravenous injection of an iodinated contrast agent and voxel-wise measurement of attenuation coefficient as a function of time (155). In the clinical setting, the accessibility and the fast scanning speed of CT makes it the first choice for making treatment decisions for ischemic stroke. BBB disruption can potentially be assessed by incorporating a DCE-CT protocol into the initial CT imaging of a patient. Recently, Park et al. developed a new *in vivo* micro-CT which uses iopromide to visualize the leakage of BBB. The new micro-CT BBB imaging technique has a high resolution and sensitivity (156).

Although some other imaging techniques (such as PET and optical imaging) have been also used to evaluate BBB permeability, their limitations, such as low resolution and inter-rater reliability, restrict their application in the clinic setting (157, 158).

## CONCLUSIONS AND PERSPECTIVE

Reperfusion therapies are critically time dependent. The earlier treatment within time windows leads to more benefits. For the patients reached beyond the time windows, “tissue window” should be considered. Emerging evidence from recent clinical trials have recognized that tissue viability defined by the imaging modalities might be a more precise and reliable surrogate marker than time window (159). The newly issued guidelines have recommended evaluation of the penumbra or infarction by DWI, PWI, and CTP to expand eligibility for mechanical thrombectomy in the 6–24 h window after stroke onset. Compared to PDM, the novel imaging features on metabolism and pathophysiology, are more specific and sensitive to examine the salvageable tissue after stroke, and show great potential to define the therapeutic window. However, there are still challenges and controversies. Nonetheless, it needs to be said, that there is no reliable setting to determine the viability of brain tissue in the acute stage of stroke. Although visibility of such imaging setting

as oxygen challenge MRI and DCE-MRI/CT for the detection of BBB leakage were tested in rodent studies, their usefulness for clinic have not been evaluated yet. Others, such as pH-weighted imaging and glutamate imaging, have only been validated in human studies, but all the same the utility of the concepts have not been evaluated in clinical trials yet (Figure 5). Though PDM tempts us to differentiate the potential salvageable tissue from infarction, unfortunately, the ideal imaging parameters and their accuracy remain elusive. Definitive validation is necessary in the future research and clinical trials. And because of a lack of standardization, the incorporation of the imaging modalities in clinical practice will be consequently limited. Future investigations on standardization of the imaging sequences and parameters to define tissue window are expected. Besides, the restricted attainability and long time needed for examination are burdens that limit PDM application for stroke patients. For instance, in Europe on average only 4% of the decision in regards of possible treatment will be based on MR perfusion and this number varied greatly from country to country (160). The time needed for an MRI perfusion scan is ~16 min. That is longer than 10 min, which are needed for CTP. However, it is possible to standardized stroke MRI protocols and reduce time in this way down to 10 min or even to 6 min by using echo planar imaging at 3 T (161). It is clear that with increased availability and standardization of the parameters, PDM could become the prime imaging technique able to precisely define the tissue window and identify patients eligible for endovascular thrombectomy.

## AUTHOR CONTRIBUTIONS

JL, QH, YL, and XH wrote the manuscript. DL and JZ made suggestions for improvement. QM and LZ created the figures. AM edited the language. All authors read, revised, and approved the final manuscript.

## FUNDING

This research was supported by the National Natural Science Foundation of China No. 82071283 to QH, China Postdoctoral Science Foundation Grant No. 2018M632130 to JL, and the National Institutes of Health P01 NS082124 to JZ.

## REFERENCES

1. Yang SH, Liu R. Four decades of ischemic penumbra and its implication for ischemic stroke. *Transl Stroke Res.* (2021). doi: 10.1007/s12975-021-00916-2. [Epub ahead of print].
2. Lapchak PA. Critical early thrombolytic and endovascular reperfusion therapy for acute ischemic stroke victims: a call for adjunct neuroprotection. *Transl Stroke Res.* (2015) 6:345–54. doi: 10.1007/s12975-015-0419-5
3. Thomalla G, Simonsen CZ, Boutitie F, Andersen G, Berthezene Y, Cheng B, et al. Wake up-mri-guided thrombolysis for stroke with unknown time of onset. *N Engl J Med.* (2018) 379:611–22. doi: 10.1056/NEJMoa1804355
4. Amiri H, Bluhmki E, Bendszus M, Eschenfelder CC, Donnan GA, Leys D, et al. European cooperative acute stroke study-4: extending the time for thrombolysis in emergency neurological deficits ecass-4: extend. *Int J Stroke.* (2016) 11:260–7. doi: 10.1177/1747493015620805
5. Nogueira RG, Jadhav AP, Haussen DC, Bonafe A, Budzik RF, Bhuva P, et al. Thrombectomy 6 to 24 hours after stroke with a mismatch between deficit and infarct. *N Engl J Med.* (2018) 378:11–21. doi: 10.1056/NEJMoa1706442
6. Albers GW, Marks MP, Lansberg MG. DEFUSE 3-Thrombectomy for stroke with selection by perfusion imaging. *N Engl J Med.* (2018) 378:708–18. doi: 10.1056/NEJMoa1713973
7. Yang SH, Lou M, Luo B, Jiang WJ, Liu R. Precision medicine for ischemic stroke, let us move beyond time is brain. *Transl Stroke Res.* (2018) 9:93–5. doi: 10.1007/s12975-017-0566-y
8. Hacke W. A new dawn for imaging-based selection in the treatment of acute stroke. *N Engl J Med.* (2018) 378:81–3. doi: 10.1056/NEJMe1713367
9. Dehkharghani S, Andre J. Imaging approaches to stroke and neurovascular disease. *Neurosurgery.* (2017) 80:681–700. doi: 10.1093/neuros/nyw108

10. Scheldeman L, Wouters A, Boutitie F, Dupont P, Christensen S, Cheng B, et al. Different mismatch concepts for magnetic resonance imaging-guided thrombolysis in unknown onset stroke. *Ann Neurol.* (2020) 87:931–8. doi: 10.1002/ana.25730
11. Astrup J, Siesjo BK, Symon L. Thresholds in cerebral ischemia - the ischemic penumbra. *Stroke.* (1981) 12:723–5. doi: 10.1161/01.STR.12.6.723
12. Iglesias-Rey R, Rodriguez-Yanez M, Rodriguez-Castro E, Pumar JM, Arias S, Santamaria M, et al. Worse outcome in stroke patients treated with rtpa without early reperfusion: associated factors. *Transl Stroke Res.* (2018) 9:347–55. doi: 10.1007/s12975-017-0584-9
13. Ahnstedt H, Sweet J, Cruden P, Bishop N, Cipolla MJ. Effects of early post-ischemic reperfusion and tpa on cerebrovascular function and nitrosative stress in female rats. *Transl Stroke Res.* (2016) 7:228–38. doi: 10.1007/s12975-016-0468-4
14. Goyal M, Ospel JM, Menon B, Almekhlafi M, Jayaraman M, Fiehler J, et al. Challenging the ischemic core concept in acute ischemic stroke imaging. *Stroke.* (2020) 51:3147–55. doi: 10.1161/STROKEAHA.120.030620
15. Gomez CR. Editorial: time is brain! *J Stroke Cerebrovasc Dis.* (1993) 3:1–2. doi: 10.1016/S1052-3057(10)80125-9
16. Mikulik R, Wahlgren N. Treatment of acute stroke: an update. *J Intern Med.* (2015) 278:145–65. doi: 10.1111/joim.12387
17. Wadiwala MF, Kamal AK. Extending the window for thrombolysis in acute stroke. *J Pak Med Assoc.* (2012) 62:858–9.
18. Desilles JP, Consoli A, Redjem H, Coskun O, Ciccio G, Smajda S, et al. Successful reperfusion with mechanical thrombectomy is associated with reduced disability and mortality in patients with pretreatment diffusion-weighted imaging-alberta stroke program early computed tomography score  $\leq 6$ . *Stroke.* (2017) 48:963–9. doi: 10.1161/STROKEAHA.116.015202
19. National Institute of Neurological Disorders, Stroke rt-PA Stroke Study Group. Tissue plasminogen activator for acute ischemic stroke. *N Engl J Med.* (1995) 333:1581–7. doi: 10.1056/NEJM199512143332401
20. Hacke W, Kaste M, Bluhmki E, Brozman M, Davalos A, Guidetti D, et al. Thrombolysis with alteplase 3 to 45 hours after acute ischemic stroke. *N Engl J Med.* (2008) 359:1317–29. doi: 10.1056/NEJMoa0804656
21. Miller DJ, Simpson JR, Silver B. Safety of thrombolysis in acute ischemic stroke: a review of complications, risk factors, and newer technologies. *Neurohospitalist.* (2011) 1:138–47. doi: 10.1177/1941875211408731
22. Ma H, Campbell BCV, Parsons MW, Churilov L, Levi CR, Hsu C, et al. Thrombolysis guided by perfusion imaging up to 9 hours after onset of stroke. *N Engl J Med.* (2019) 380:1795–803. doi: 10.1056/NEJMoa1813046
23. Sykora M, Kellert L, Michel P, Eskandari A, Feil K, Remi J, et al. Thrombolysis in stroke with unknown onset based on non-contrast computerized tomography (trust ct). *J Am Heart Assoc.* (2020) 9:e014265. doi: 10.1161/JAHA.119.014265
24. Powers WJ, Rabinstein AA, Ackerson T, Adeoye OM, Bambakidis NC, Becker K, et al. Guidelines for the early management of patients with acute ischemic stroke: 2019 update to the 2018 guidelines for the early management of acute ischemic stroke: a guideline for healthcare professionals from the american heart association/american stroke association. *Stroke.* (2019) 50:e344–418. doi: 10.1161/STR.0000000000000211
25. Katsanos AH, Safouris A, Sarraj A, Magoufis G, Leker RR, Khatri P, et al. Intravenous thrombolysis with tenecteplase in patients with large vessel occlusions: systematic review and meta-analysis. *Stroke.* (2021) 52:308–12. doi: 10.1161/STROKEAHA.120.030220
26. Saver JL, Goyal M, Bonafe A, Diener HC, Levy EI, Pereira VM, et al. Stent-retriever thrombectomy after intravenous t-pa vs. T-pa alone in stroke. *N Engl J Med.* (2015) 372:2285–95. doi: 10.1056/NEJMoa1415061
27. Campbell BC, Mitchell PJ, Kleinig TJ, Dewey HM, Churilov L, Yassi N, et al. (Extend-ia) endovascular therapy for ischemic stroke with perfusion-imaging selection. *N Engl J Med.* (2015) 372:1009–18. doi: 10.1056/NEJMoa1414792
28. Berkhemer OA, Fransen PS, Beumer D, van den Berg LA, Lingsma HF, Yoo AJ, et al. Mr clean-a randomized trial of intraarterial treatment for acute ischemic stroke. *N Engl J Med.* (2015) 372:11–20. doi: 10.1056/NEJMoa1411587
29. Jovin TG, Chamorro A, Cobo E, de Miquel MA, Molina CA, Rovira A, et al. Revascat-thrombectomy within 8 hours after symptom onset in ischemic stroke. *N Engl J Med.* (2015) 372:2296–306. doi: 10.1056/NEJMoa1503780
30. Goyal M, Demchuk AM, Menon BK, Eesa M, Rempel JL, Thornton J, et al. Randomized assessment of rapid endovascular treatment of ischemic stroke. *N Engl J Med.* (2015) 372:1019–30. doi: 10.1056/NEJMoa1414905
31. Motyer R, Thornton J, Power S, Brennan P, O'Hare A, Looby S, et al. Endovascular thrombectomy beyond 12 hours of stroke onset: a stroke network's experience of late intervention. *J Neurointerv Surg.* (2018) 10:1043–6. doi: 10.1136/neurintsurg-2017-013575
32. Gunawardena R, Cheung A, Spira P, He J, Wenderoth J, Chiu AHY. Successful endovascular thrombectomy 90h after stroke onset. *J Clin Neurosci.* (2017) 46:69–71. doi: 10.1016/j.jocn.2017.08.047
33. Janjua N, Farkas J. Thrombectomy for delayed basilar stent occlusion with good outcome. *J Vasc Interv Neurol.* (2013) 6:19–24.
34. McBride DW, Wu G, Nowrangi D, Flores JJ, Hui L, Krafft PR, et al. Delayed recanalization promotes functional recovery in rats following permanent middle cerebral artery occlusion. *Transl Stroke Res.* (2018) 9:185–98. doi: 10.1007/s12975-018-0610-6
35. Astrup J, Symon L, Branston NM, Lassen NA. Cortical evoked potential and extracellular k<sup>+</sup> and h<sup>+</sup> at critical levels of brain ischemia. *Stroke.* (1977) 8:51–7. doi: 10.1161/01.STR.8.1.51
36. Baron JC, Bousser MG, Rey A, Guillard A, Comar D, Castaigne P. Reversal of focal "misery-perfusion syndrome" by extra-intracranial arterial bypass in hemodynamic cerebral ischemia. A case study with 15o positron emission tomography. *Stroke.* (1981) 12:454–9. doi: 10.1161/01.STR.12.4.454
37. Heiss WD. Ischemic penumbra: evidence from functional imaging in man. *J Cereb Blood Flow Metab.* (2000) 20:1276–93. doi: 10.1097/00004647-200009000-00002
38. Powers WJ, Grubb RL Jr, Darriet D, Raichle ME. Cerebral blood flow and cerebral metabolic rate of oxygen requirements for cerebral function and viability in humans. *J Cereb Blood Flow Metab.* (1985) 5:600–8. doi: 10.1038/jcbfm.1985.89
39. Heiss WD, Graf R, Wienhard K, Lottgen J, Saito R, Fujita T, et al. Dynamic penumbra demonstrated by sequential multitracer pet after middle cerebral artery occlusion in cats. *J Cereb Blood Flow Metab.* (1994) 14:892–902. doi: 10.1038/jcbfm.1994.120
40. Baron JC. Mapping the ischaemic penumbra with pet: Implications for acute stroke treatment. *Cerebrovasc Dis.* (1999) 9:193–201. doi: 10.1159/000015955
41. Marchal G, Benali K, Iglesias S, Viader F, Derlon JM, Baron JC. Voxel-based mapping of irreversible ischaemic damage with pet in acute stroke. *Brain.* (1999) 122:2387–400. doi: 10.1093/brain/122.12.2387
42. Baron JC. Perfusion thresholds in human cerebral ischemia: historical perspective and therapeutic implications. *Cerebrovasc Dis.* (2001) 11 Suppl 1:2–8. doi: 10.1159/000049119
43. Zaro-Weber O, Fleischer H, Reiblich L, Schuster A, Moeller-Hartmann W, Heiss WD. Penumbra detection in acute stroke with perfusion magnetic resonance imaging: validation with (15) o-positron emission tomography. *Ann Neurol.* (2019) 85:875–86. doi: 10.1002/ana.25479
44. Sobesky J. Refining the mismatch concept in acute stroke: lessons learned from pet and mri. *J Cereb Blood Flow Metab.* (2012) 32:1416–25. doi: 10.1038/jcbfm.2012.54
45. Rother J, Schellinger PD, Gass A, Siebler M, Villringer A, Fiebich JB, et al. Effect of intravenous thrombolysis on mri parameters and functional outcome in acute stroke  $< 6$  hours. *Stroke.* (2002) 33:2438–45. doi: 10.1161/01.STR.0000030109.12281.23
46. Duong TQ, Fisher M. Applications of diffusion/perfusion magnetic resonance imaging in experimental and clinical aspects of stroke. *Curr Atheroscler Rep.* (2004) 6:267–73. doi: 10.1007/s11883-004-0057-y
47. Ford AL, An H, Kong L, Zhu H, Vo KD, Powers WJ, et al. Clinically relevant reperfusion in acute ischemic stroke: Mtt performs better than tmax and ttp. *Transl Stroke Res.* (2014) 5:415–21. doi: 10.1007/s12975-014-0325-2
48. Schellinger PD, Fiebich JB, Jansen O, Ringleb PA, Mohr A, Steiner T, et al. Stroke magnetic resonance imaging within 6 hours after onset of hyperacute cerebral ischemia. *Ann Neurol.* (2001) 49:460–9. doi: 10.1002/ana.95
49. Muller TB, Haraldseth O, Jones RA, Sebastiani G, Godtliebsen F, Lindboe CF, et al. Combined perfusion and diffusion-weighted magnetic resonance

- imaging in a rat model of reversible middle cerebral artery occlusion. *Stroke*. (1995) 26:451–7. doi: 10.1161/01.STR.26.3.451
50. Kohno K, Hoehn-Berlage M, Mies G, Back T, Hossmann KA. Relationship between diffusion-weighted mr images, cerebral blood flow, and energy state in experimental brain infarction. *Magn Reson Imaging*. (1995) 13:73–80. doi: 10.1016/0730-725X(94)00080-M
  51. Schlaug G, Benfield A, Baird AE, Siewert B, Lovblad KO, Parker RA, et al. The ischemic penumbra: operationally defined by diffusion and perfusion mri. *Neurology*. (1999) 53:1528–37. doi: 10.1212/WNL.53.7.1528
  52. Singer OC, Du Mesnil De Rochemont R, Foerch C, Stengel A, Sitzer M, Lanfermann H, et al. Early functional recovery and the fate of the diffusion/perfusion mismatch in patients with proximal middle cerebral artery occlusion. *Cerebrovasc Dis*. (2004) 17:13–20. doi: 10.1159/000073893
  53. Baird AE, Lovblad KO, Dashe JF, Connor A, Burzynski C, Schlaug G, et al. Clinical correlations of diffusion and perfusion lesion volumes in acute ischemic stroke. *Cerebrovasc Dis*. (2000) 10:441–8. doi: 10.1159/000016105
  54. Albers GW, Thijs VN, Wechsler L, Kemp S, Schlaug G, Skalabrin E, et al. Magnetic resonance imaging profiles predict clinical response to early reperfusion: the diffusion and perfusion imaging evaluation for understanding stroke evolution (defuse) study. *Ann Neurol*. (2006) 60:508–17. doi: 10.1002/ana.20976
  55. Davis SM, Donnan GA, Parsons MW, Levi C, Butcher KS, Peeters A, et al. Effects of alteplase beyond 3 h after stroke in the echoplanar imaging thrombolytic evaluation trial (epithet): a placebo-controlled randomised trial. *Lancet Neurol*. (2008) 7:299–309. doi: 10.1016/S1474-4422(08)70044-9
  56. Sobesky J, Zaro Weber O, Lehnhardt FG, Hesselmann V, Neveling M, Jacobs A, et al. Does the mismatch match the penumbra? Magnetic resonance imaging and positron emission tomography in early ischemic stroke. *Stroke*. (2005) 36:980–5. doi: 10.1161/01.STR.0000160751.79241.a3
  57. Heiss WD, Sobesky J, Hesselmann V. Identifying thresholds for penumbra and irreversible tissue damage. *Stroke*. (2004) 35:2671–4. doi: 10.1161/01.STR.0000143329.81997.8a
  58. Dani KA, Thomas RG, Chappell FM, Shuler K, MacLeod MJ, Muir KW, et al. Computed tomography and magnetic resonance perfusion imaging in ischemic stroke: definitions and thresholds. *Ann Neurol*. (2011) 70:384–401. doi: 10.1002/ana.22550
  59. Hussain MS, Bhagat YA, Liu S, Scozzafava J, Khan KA, Dillon WP, et al. Dwi lesion volume reduction following acute stroke treatment with transient partial aortic obstruction. *J Neuroimaging*. (2010) 20:379–81. doi: 10.1111/j.1552-6569.2009.00407.x
  60. Kidwell CS, Alger JR, Saver JL. Beyond mismatch: evolving paradigms in imaging the ischemic penumbra with multimodal magnetic resonance imaging. *Stroke*. (2003) 34:2729–35. doi: 10.1161/01.STR.0000097608.38779.CC
  61. Rivers CS, Wardlaw JM, Armitage PA, Bastin ME, Carpenter TK, Cvorovic V, et al. Do acute diffusion- and perfusion-weighted mri lesions identify final infarct volume in ischemic stroke? *Stroke*. (2006) 37:98–104. doi: 10.1161/01.STR.0000195197.66606.bb
  62. Powers WJ. Perfusion-diffusion mismatch: does it identify who will benefit from reperfusion therapy? *Transl Stroke Res*. (2012) 3:182–7. doi: 10.1007/s12975-012-0160-2
  63. Davis SM, Donnan GA. Mr mismatch and thrombolysis: appealing but validation required. *Stroke*. (2009) 40:2910. doi: 10.1161/STROKEAHA.109.552893
  64. Wardlaw JM. Surrogate outcomes: a cautionary note. *Stroke*. (2009) 40:1029–31. doi: 10.1161/STROKEAHA.108.540641
  65. Wetterling F, Gallagher L, Mullin J, Holmes WM, McCabe C, Macrae IM, et al. Sodium-23 magnetic resonance imaging has potential for improving penumbra detection but not for estimating stroke onset time. *J Cereb Blood Flow Metab*. (2015) 35:103–10. doi: 10.1038/jcbfm.2014.174
  66. Wetterling F, Chatzikonstantinou E, Tritschler L, Meairs S, Fatar M, Schad LR, et al. Investigating potentially salvageable penumbra tissue in an in vivo model of transient ischemic stroke using sodium, diffusion, and perfusion magnetic resonance imaging. *BMC Neurosci*. (2016) 17:82. doi: 10.1186/s12868-016-0316-1
  67. Boada FE, Qian Y, Nemoto E, Jovin T, Jungreis C, Jones SC, et al. Sodium mri and the assessment of irreversible tissue damage during hyper-acute stroke. *Transl Stroke Res*. (2012) 3:236–45. doi: 10.1007/s12975-012-0168-7
  68. Wang Y, Hu W, Perez-Trepichio AD, Ng TC, Furlan AJ, Majors AW, et al. Brain tissue sodium is a ticking clock telling time after arterial occlusion in rat focal cerebral ischemia. *Stroke*. (2000) 31:1386–91. doi: 10.1161/01.STR.31.6.1386
  69. Chalian M, Tekes A, Meoded A, Poretti A, Huisman TA. Susceptibility-weighted imaging (swi): a potential non-invasive imaging tool for characterizing ischemic brain injury? *J Neuroradiol*. (2011) 38:187–90. doi: 10.1016/j.neurad.2010.12.006
  70. Luo S, Yang L, Wang L. Comparison of susceptibility-weighted and perfusion-weighted magnetic resonance imaging in the detection of penumbra in acute ischemic stroke. *J Neuroradiol*. (2015) 42:255–60. doi: 10.1016/j.neurad.2014.07.002
  71. Robertson CA, McCabe C, Lopez-Gonzalez MR, Deuchar GA, Dani K, Holmes WM, et al. Detection of ischemic penumbra using combined perfusion and t2\* oxygen challenge imaging. *Int J Stroke*. (2015) 10:42–50. doi: 10.1111/ijvs.12327
  72. Zhu G, Michel P, Zhang W, Wintermark M. Standardization of stroke perfusion ct for reperfusion therapy. *Transl Stroke Res*. (2012) 3:221–7. doi: 10.1007/s12975-012-0156-y
  73. Wintermark M, Albers GW, Alexandrov AV, Alger JR, Bammer R, Baron JC, et al. Acute stroke imaging research roadmap. *Stroke*. (2008) 39:1621–8. doi: 10.1161/STROKEAHA.107.512319
  74. Zhu G, Jovin T, Aghaebrahim A, Michel P, Zhang W, Wintermark M. Does perfusion imaging add value compared with plain parenchymal and vascular imaging? *J Neurointerv Surg*. (2012) 4:246–50. doi: 10.1136/neurintsurg-2012-010416
  75. Alves JE, Carneiro A, Xavier J. Reliability of ct perfusion in the evaluation of the ischaemic penumbra. *Neuroradiol J*. (2014) 27:91–5. doi: 10.15274/NRJ-2014-10010
  76. Hossmann KA. Viability thresholds and the penumbra of focal ischemia. *Ann Neurol*. (1994) 36:557–65. doi: 10.1002/ana.410360404
  77. Kiewert C, Mdzinarishvili A, Hartmann J, Bickel U, Klein J. Metabolic and transmitter changes in core and penumbra after middle cerebral artery occlusion in mice. *Brain Res*. (2010) 1312:101–7. doi: 10.1016/j.brainres.2009.11.068
  78. Galeffi F, Sinnar S, Schwartz-Bloom RD. Diazepam promotes atp recovery and prevents cytochrome c release in hippocampal slices after in vitro ischemia. *J Neurochem*. (2000) 75:1242–9. doi: 10.1046/j.1471-4159.2000.0751242.x
  79. Kuroiwa T, Mies G, Hermann D, Hakamata Y, Hanyu S, Ito U. Regional differences in the rate of energy impairment after threshold level ischemia for induction of cerebral infarction in gerbils. *Acta Neuropathol*. (2000) 100:587–94. doi: 10.1007/s004010000235
  80. Hata R, Maeda K, Hermann D, Mies G, Hossmann KA. Evolution of brain infarction after transient focal cerebral ischemia in mice. *J Cereb Blood Flow Metab*. (2000) 20:937–46. doi: 10.1097/00004647-200006000-00006
  81. Welsh FA, Marcy VR, Sims RE. Nadh fluorescence and regional energy metabolites during focal ischemia and reperfusion of rat brain. *J Cereb Blood Flow Metab*. (1991) 11:459–65. doi: 10.1038/jcbfm.1991.88
  82. Wang Z, Mascarenhas C, Jia X. Positron emission tomography after ischemic brain injury: current challenges and future developments. *Transl Stroke Res*. (2020) 11:628–42. doi: 10.1007/s12975-019-00765-0
  83. Baron JC, Jones T. Oxygen metabolism, oxygen extraction and positron emission tomography: historical perspective and impact on basic and clinical neuroscience. *Neuroimage*. (2012) 61:492–504. doi: 10.1016/j.neuroimage.2011.12.036
  84. Heiss WD. The ischemic penumbra: correlates in imaging and implications for treatment of ischemic stroke. The johann jacob wepfer award 2011. *Cerebrovasc Dis*. (2011) 32:307–20. doi: 10.1159/000330462
  85. Jones T, Chesler DA, Ter-Pogossian MM. The continuous inhalation of oxygen-15 for assessing regional oxygen extraction in the brain of man. *Br J Radiol*. (1976) 49:339–43. doi: 10.1259/0007-1285-49-580-339
  86. Heiss WD, Grund M, Thiel A, von Stockhausen HM, Rudolf J, Ghaemi M, et al. Tissue at risk of infarction rescued by early reperfusion: a positron emission tomography study in systemic recombinant tissue plasminogen activator thrombolysis of acute stroke. *J Cereb Blood Flow Metab*. (1998) 18:1298–307. doi: 10.1097/00004647-199812000-00004

87. Lin W, Powers WJ. Oxygen metabolism in acute ischemic stroke. *J Cereb Blood Flow Metab.* (2018) 38:1481–99. doi: 10.1177/0271678X17722095
88. Treyer V, Jobin M, Burger C, Teneggi V, Buck A. Quantitative cerebral h2(15)o perfusion pet without arterial blood sampling, a method based on washout rate. *Eur J Nucl Med Mol Imaging.* (2003) 30:572–80. doi: 10.1007/s00259-002-1105-x
89. Kudomi N, Hirano Y, Koshino K, Hayashi T, Watabe H, Fukushima K, et al. Rapid quantitative cbf and cmro(2) measurements from a single pet scan with sequential administration of dual (15)o-labeled tracers. *J Cereb Blood Flow Metab.* (2013) 33:440–8. doi: 10.1038/jcbfm.2012.188
90. Kudomi N, Maeda Y, Yamamoto H, Yamamoto Y, Hatakeyama T, Nishiyama Y. Reconstruction of input functions from a dynamic pet image with sequential administration of (15)o2 and [formula: See text] for noninvasive and ultra-rapid measurement of cbf, oef, and cmro2. *J Cereb Blood Flow Metab.* (2018) 38:780–92. doi: 10.1177/0271678X17713574
91. Magata Y, Temma T, Iida H, Ogawa M, Mukai T, Iida Y, et al. Development of injectable o-15 oxygen and estimation of rat oef. *J Cereb Blood Flow Metab.* (2003) 23:671–6. doi: 10.1097/01.WCB.0000066792.97069.B3
92. Temma T, Koshino K, Moriguchi T, Enmi J, Iida H. Pet quantification of cerebral oxygen metabolism in small animals. *ScientificWorldJournal.* (2014) 2014:159103. doi: 10.1155/2014/159103
93. Tiwari VN, Kiyono Y, Kobayashi M, Mori T, Kudo T, Okazawa H, et al. Automatic labeling method for injectable 15o-oxygen using hemoglobin-containing liposome vesicles and its application for measurement of brain oxygen consumption by pet. *Nucl Med Biol.* (2010) 37:77–83. doi: 10.1016/j.nucmedbio.2009.08.004
94. Heiss WD, Graf R, Fujita T, Ohta K, Bauer B, Lottgen J, et al. Early detection of irreversibly damaged ischemic tissue by flumazenil positron emission tomography in cats. *Stroke.* (1997) 28:2045–51. doi: 10.1161/01.STR.28.10.2045
95. Heiss WD, Kracht L, Grond M, Rudolf J, Bauer B, Wienhard K, et al. Early [(11)c]flumazenil/h(2)o positron emission tomography predicts irreversible ischemic cortical damage in stroke patients receiving acute thrombolytic therapy. *Stroke.* (2000) 31:366–9. doi: 10.1161/01.STR.31.2.366
96. Thiel A, Lottgen J, Grond M, Pietrzyk U, Heiss WD. Estimation of regional cerebral blood flow levels in ischemia using [(15)o]water of [(11)c]flumazenil pet without arterial input function. *J Comput Assist Tomogr.* (2001) 25:446–51. doi: 10.1097/00004728-200105000-00019
97. Rojas S, Martin A, Pareto D, Herance JR, Abad S, Ruiz A, et al. Positron emission tomography with 11c-flumazenil in the rat shows preservation of binding sites during the acute phase after 2 h-transient focal ischemia. *Neuroscience.* (2011) 182:208–16. doi: 10.1016/j.neuroscience.2011.03.013
98. Takasawa M, Moustafa RR, Baron JC. Applications of nitroimidazole *in vivo* hypoxia imaging in ischemic stroke. *Stroke.* (2008) 39:1629–37. doi: 10.1161/STROKEAHA.107.485938
99. Takasawa M, Beech JS, Fryer TD, Jones PS, Ahmed T, Smith R, et al. Single-subject statistical mapping of acute brain hypoxia in the rat following middle cerebral artery occlusion: a micropet study. *Exp Neurol.* (2011) 229:251–8. doi: 10.1016/j.expneurol.2011.02.005
100. Lee GH, Kim JS, Oh SJ, Kang DW, Kim JS, Kwon SU. (18)f-fluoromisonidazole (fmiso) positron emission tomography (pet) predicts early infarct growth in patients with acute ischemic stroke. *J Neuroimaging.* (2015) 25:652–5. doi: 10.1111/jon.12180
101. Falcao AL, Reutens DC, Markus R, Koga M, Read SJ, Tochon-Danguy H, et al. The resistance to ischemia of white and gray matter after stroke. *Ann Neurol.* (2004) 56:695–701. doi: 10.1002/ana.20265
102. Markus R, Reutens DC, Kazui S, Read S, Wright P, Pearce DC, et al. Hypoxic tissue in ischaemic stroke: persistence and clinical consequences of spontaneous survival. *Brain.* (2004) 127:1427–36. doi: 10.1093/brain/awh162
103. Lewis JS, Herrero P, Sharp TL, Engelbach JA, Fujibayashi Y, Laforest R, et al. Delineation of hypoxia in canine myocardium using pet and copper(ii)-diacetyl-bis(n(4)-methylthiosemicarbazone). *J Nucl Med.* (2002) 43:1557–69.
104. Huuskonen MT, Tuo QZ, Loppi S, Dhungana H, Korhonen P, McInnes LE, et al. The copper bis(thiosemicarbazone) complex cu(ii)(atsm) is protective against cerebral ischemia through modulation of the inflammatory milieu. *Neurotherapeutics.* (2017) 14:519–32. doi: 10.1007/s13311-016-0504-9
105. van der Toorn A, Verheul HB, Berkelbach van der Sprenkel JW, Tulleken CA, Nicolay K. Changes in metabolites and tissue water status after focal ischemia in cat brain assessed with localized proton mr spectroscopy. *Magn Reson Med.* (1994) 32:685–91. doi: 10.1002/mrm.1910320602
106. Sager TN, Laursen H, Hansen AJ. Changes in n-acetyl-aspartate content during focal and global brain ischemia of the rat. *J Cereb Blood Flow Metab.* (1995) 15:639–46. doi: 10.1038/jcbfm.1995.79
107. Jimenez-Xarrie E, Davila M, Gil-Perotin S, Jurado-Rodriguez A, Candiota AP, Delgado-Mederos R, et al. *In vivo* and *ex vivo* magnetic resonance spectroscopy of the infarct and the subventricular zone in experimental stroke. *J Cereb Blood Flow Metab.* (2015) 35:828–34. doi: 10.1038/jcbfm.2014.257
108. Saunders DE. Mr spectroscopy in stroke. *Br Med Bull.* (2000) 56:334–45. doi: 10.1258/0007142001903256
109. Bruhn H, Frahm J, Gyngell ML, Merboldt KD, Hanicke W, Sauter R. Cerebral metabolism in man after acute stroke: new observations using localized proton nmr spectroscopy. *Magn Reson Med.* (1989) 9:126–31. doi: 10.1002/mrm.1910090115
110. Wardlaw JM, Marshall I, Wild J, Dennis MS, Cannon J, Lewis SC. Studies of acute ischemic stroke with proton magnetic resonance spectroscopy: relation between time from onset, neurological deficit, metabolite abnormalities in the infarct, blood flow, and clinical outcome. *Stroke.* (1998) 29:1618–24. doi: 10.1161/01.STR.29.8.1618
111. Parsons MW, Li T, Barber PA, Yang Q, Darby DG, Desmond PM, et al. Combined (1)h mr spectroscopy and diffusion-weighted mri improves the prediction of stroke outcome. *Neurology.* (2000) 55:498–505. doi: 10.1212/WNL.55.4.498
112. Klijn CJ, Kappelle LJ, van der Grond J, Algra A, Tulleken CA, van Gijn J. Magnetic resonance techniques for the identification of patients with symptomatic carotid artery occlusion at high risk of cerebral ischemic events. *Stroke.* (2000) 31:3001–7. doi: 10.1161/01.STR.31.12.3001
113. Cheung JS, Wang X, Zhe Sun P. Magnetic resonance characterization of ischemic tissue metabolism. *Open Neuroimag J.* (2011) 5:66–73. doi: 10.2174/1874440001105010066
114. Komatsumoto S, Nioka S, Greenberg JH, Yoshizaki K, Subramanian VH, Chance B, et al. Cerebral energy metabolism measured *in vivo* by 31p-nmr in middle cerebral artery occlusion in the cat—relation to severity of stroke. *J Cereb Blood Flow Metab.* (1987) 7:557–62. doi: 10.1038/jcbfm.1987.105
115. Germano IM, Pitts LH, Berry I, De Armond SJ. High energy phosphate metabolism in experimental permanent focal cerebral ischemia: an *in vivo* 31p magnetic resonance spectroscopy study. *J Cereb Blood Flow Metab.* (1988) 8:24–31. doi: 10.1038/jcbfm.1988.4
116. Shen Q, Huang S, Duong TQ. T2\*-weighted fmri time-to-peak of oxygen challenge in ischemic stroke. *J Cereb Blood Flow Metab.* (2016) 36:283–91. doi: 10.1177/0271678X15606461
117. Shen Q, Huang S, Du F, Duong TQ. Probing ischemic tissue fate with bold fmri of brief oxygen challenge. *Brain Res.* (2011) 1425:132–41. doi: 10.1016/j.brainres.2011.09.052
118. Deuchar GA, Brennan D, Griffiths H, Macrae IM, Santosh C. Perfluorocarbons enhance a t2\*-based mri technique for identifying the penumbra in a rat model of acute ischemic stroke. *J Cereb Blood Flow Metab.* (2013) 33:1422–8. doi: 10.1038/jcbfm.2013.86
119. Deuchar GA, Brennan D, Holmes WM, Shaw M, Macrae IM, Santosh C. Perfluorocarbon enhanced glasgow oxygen level dependent (gold) magnetic resonance metabolic imaging identifies the penumbra following acute ischemic stroke. *Theranostics.* (2018) 8:1706–22. doi: 10.7150/thno.21685
120. Deuchar GA, van Kralingen JC, Work LM, Santosh C, Muir KW, McCabe C, et al. Preclinical validation of the therapeutic potential of glasgow oxygen level dependent (gold) technology: a theranostic for acute stroke. *Transl Stroke Res.* (2019) 10:583–95. doi: 10.1007/s12975-018-0679-y
121. Zhou J, Payen JF, Wilson DA, Traystman RJ, van Zijl PC. Using the amide proton signals of intracellular proteins and peptides to detect ph effects in mri. *Nat Med.* (2003) 9:1085–90. doi: 10.1038/nm907
122. Cheung J, Doerr M, Hu R, Sun PZ. Refined ischemic penumbra imaging with tissue ph and diffusion kurtosis magnetic resonance imaging. *Transl Stroke Res.* (2020). doi: 10.1007/s12975-020-00868-z. [Epub ahead of print].
123. Sun PZ, Cheung JS, Wang E, Lo EH. Association between ph-weighted endogenous amide proton chemical exchange saturation transfer mri and

- tissue lactic acidosis during acute ischemic stroke. *J Cereb Blood Flow Metab.* (2011) 31:1743–50. doi: 10.1038/jcbfm.2011.23
124. Sun PZ, Zhou J, Sun W, Huang J, van Zijl PC. Detection of the ischemic penumbra using ph-weighted mri. *J Cereb Blood Flow Metab.* (2007) 27:1129–36. doi: 10.1038/sj.jcbfm.9600424
  125. Jokivarsi KT, Hiltunen Y, Tuunanen PI, Kauppinen RA, Grohn OH. Correlating tissue outcome with quantitative multiparametric mri of acute cerebral ischemia in rats. *J Cereb Blood Flow Metab.* (2010) 30:415–27. doi: 10.1038/jcbfm.2009.236
  126. Tietze A, Blicher J, Mikkelsen IK, Ostergaard L, Strother MK, Smith SA, et al. Assessment of ischemic penumbra in patients with hyperacute stroke using amide proton transfer (apt) chemical exchange saturation transfer (cest) mri. *NMR Biomed.* (2014) 27:163–74. doi: 10.1002/nbm.3048
  127. Harston GW, Tee YK, Blockley N, Okell TW, Thandeswaran S, Shaya G, et al. Identifying the ischaemic penumbra using ph-weighted magnetization transfer resonance imaging. *Brain.* (2015) 138:36–42. doi: 10.1093/brain/awu374
  128. Heo HY, Zhang Y, Burton TM, Jiang S, Zhao Y, van Zijl PCM, et al. Improving the detection sensitivity of ph-weighted amide proton transfer mri in acute stroke patients using extrapolated semisolid magnetization transfer reference signals. *Magn Reson Med.* (2017) 78:871–80. doi: 10.1002/mrm.26799
  129. Tee YK, Harston GW, Blockley N, Okell TW, Levman J, Sheerin F, et al. Comparing different analysis methods for quantifying the mri amide proton transfer (apt) effect in hyperacute stroke patients. *NMR Biomed.* (2014) 27:1019–29. doi: 10.1002/nbm.3147
  130. Jin T, Wang P, Hitchens TK, Kim SG. Enhancing sensitivity of ph-weighted mri with combination of amide and guanidyl cest. *Neuroimage.* (2017) 157:341–50. doi: 10.1016/j.neuroimage.2017.06.007
  131. Dani KA, Warach S. Metabolic imaging of ischemic stroke: the present and future. *Am J Neuroradiol.* (2014) 35:S37–43. doi: 10.3174/ajnr.A3789
  132. Dong S, Maniar S, Manole MD, Sun D. Cerebral hypoperfusion and other shared brain pathologies in ischemic stroke and alzheimer's disease. *Transl Stroke Res.* (2018) 9:238–50. doi: 10.1007/s12975-017-0570-2
  133. Pennypacker KR. Peripheral immune response to cns injury. *Transl Stroke Res.* (2012) 3:305. doi: 10.1007/s12975-012-0204-7
  134. Chen B, Ng G, Gao Y, Low SW, Sandanaraj E, Ramasamy B, et al. Non-invasive multimodality imaging directly shows trpm4 inhibition ameliorates stroke reperfusion injury. *Transl Stroke Res.* (2019) 10:91–103. doi: 10.1007/s12975-018-0621-3
  135. Ren Y, Li C, Chang J, Wang R, Wang Y, Chu XP. H1a as a novel neuroprotective agent for ischemic stroke by inhibition of acid-sensing ion channel 1a. *Transl Stroke Res.* (2018) 9:96–8. doi: 10.1007/s12975-017-0575-x
  136. Ramos-Cabrera P, Campos F, Sobrino T, Castillo J. Targeting the ischemic penumbra. *Stroke.* (2011) 42:S7–11. doi: 10.1161/STROKEAHA.110.596684
  137. Bivard A, Krishnamurthy V, Stanwell P, Yassi N, Spratt NJ, Nilsson M, et al. Spectroscopy of reperfused tissue after stroke reveals heightened metabolism in patients with good clinical outcomes. *J Cereb Blood Flow Metab.* (2014) 34:1944–50. doi: 10.1038/jcbfm.2014.166
  138. Cai K, Haris M, Singh A, Kogan F, Greenberg JH, Hariharan H, et al. Magnetic resonance imaging of glutamate. *Nat Med.* (2012) 18:302–6. doi: 10.1038/nm.2615
  139. Drieu A, Buendia I, Levard D, Helie P, Brodin C, Vivien D, et al. Immune responses and anti-inflammatory strategies in a clinically relevant model of thromboembolic ischemic stroke with reperfusion. *Transl Stroke Res.* (2020) 11:481–95. doi: 10.1007/s12975-019-00733-8
  140. Saleh A, Schroeter M, Jonkmanns C, Hartung HP, Modder U, Jander S. *In vivo* mri of brain inflammation in human ischaemic stroke. *Brain.* (2004) 127:1670–7. doi: 10.1093/brain/awh191
  141. Saleh A, Schroeter M, Ringelstein A, Hartung HP, Siebler M, Modder U, et al. Iron oxide particle-enhanced mri suggests variability of brain inflammation at early stages after ischemic stroke. *Stroke.* (2007) 38:2733–7. doi: 10.1161/STROKEAHA.107.481788
  142. Rausch M, Sauter A, Frohlich J, Neubacher U, Radu EW, Rudin M. Dynamic patterns of uspio enhancement can be observed in macrophages after ischemic brain damage. *Magn Reson Med.* (2001) 46:1018–22. doi: 10.1002/mrm.1290
  143. Oude Engberink RD, Blezer EL, Hoff EI, van der Pol SM, van der Toorn A, Dijkhuizen RM, et al. Mri of monocyte infiltration in an animal model of neuroinflammation using spio-labeled monocytes or free uspio. *J Cereb Blood Flow Metab.* (2008) 28:841–51. doi: 10.1038/sj.jcbfm.9600580
  144. Shichinohe H, Kuroda S, Kudo K, Ito M, Kawabori M, Miyamoto M, et al. Visualization of the superparamagnetic iron oxide (spio)-labeled bone marrow stromal cells using a 30-t mri-a pilot study for clinical testing of neurotransplantation. *Transl Stroke Res.* (2012) 3:99–106. doi: 10.1007/s12975-011-0138-5
  145. Jin AY, Tuor UI, Rushforth D, Filfil R, Kaur J, Ni F, et al. Magnetic resonance molecular imaging of post-stroke neuroinflammation with a p-selectin targeted iron oxide nanoparticle. *Contrast Media Mol Imaging.* (2009) 4:305–11. doi: 10.1002/cmim.292
  146. Barber PA, Foniok T, Kirk D, Buchan AM, Laurent S, Boutry S, et al. Mr molecular imaging of early endothelial activation in focal ischemia. *Ann Neurol.* (2004) 56:116–20. doi: 10.1002/ana.20162
  147. Hoyte LC, Brooks KJ, Nagel S, Akhtar A, Chen R, Mardiguian S, et al. Molecular magnetic resonance imaging of acute vascular cell adhesion molecule-1 expression in a mouse model of cerebral ischemia. *J Cereb Blood Flow Metab.* (2010) 30:1178–87. doi: 10.1038/jcbfm.2009.287
  148. Gulyas B, Toth M, Schain M, Airaksinen A, Vas A, Kostulas K, et al. Evolution of microglial activation in ischaemic core and perinfarct regions after stroke: a pet study with the tspo molecular imaging biomarker [(111)cv]vinpocetine. *J Neurol Sci.* (2012) 320:110–7. doi: 10.1016/j.jns.2012.06.026
  149. Bernardo-Castro S, Sousa JA, Bras A, Cecilia C, Rodrigues B, Almendra L, et al. Pathophysiology of blood-brain barrier permeability throughout the different stages of ischemic stroke and its implication on hemorrhagic transformation and recovery. *Front Neurol.* (2020) 11:594672. doi: 10.3389/fneur.2020.594672
  150. Zeynalov E, Jones SM, Elliott JP. Therapeutic time window for conivaptan treatment against stroke-evoked brain edema and blood-brain barrier disruption in mice. *PLoS ONE.* (2017) 12:e0183985. doi: 10.1371/journal.pone.0183985
  151. Jiang Q, Ewing JR, Chopp M. Mri of blood-brain barrier permeability in cerebral ischemia. *Transl Stroke Res.* (2012) 3:56–64. doi: 10.1007/s12975-011-0133-x
  152. Villringer K, Sanz Cuesta BE, Ostwaldt AC, Grittner U, Brunecker P, Khalil AA, et al. Dce-mri blood-brain barrier assessment in acute ischemic stroke. *Neurology.* (2017) 88:433–40. doi: 10.1212/WNL.00000000000003566
  153. Heye AK, Culling RD, Valdes Hernandez Mdel C, Thrippleton MJ, Wardlaw JM. Assessment of blood-brain barrier disruption using dynamic contrast-enhanced mri. A systematic review. *Neuroimage Clin.* (2014) 6:262–74. doi: 10.1016/j.nicl.2014.09.002
  154. Pillai DR, Dittmar MS, Baldaranov D, Heidemann RM, Henning EC, Schuierer G, et al. Cerebral ischemia-reperfusion injury in rats—a 3 t mri study on biphasic blood-brain barrier opening and the dynamics of edema formation. *J Cereb Blood Flow Metab.* (2009) 29:1846–55. doi: 10.1038/jcbfm.2009.106
  155. Merali Z, Wong T, Leung J, Gao MM, Mikulis D, Kassner A. Dynamic contrast-enhanced mri and ct provide comparable measurement of blood-brain barrier permeability in a rodent stroke model. *Magn Reson Imaging.* (2015) 33:1007–12. doi: 10.1016/j.mri.2015.06.021
  156. Park JY, Lee SK, Kim JY, Je KH, Schellingerhout D, Kim DE, et al. New micro-computed tomography-based high-resolution blood-brain barrier imaging technique to study ischemic stroke. *Stroke.* (2014) 45:2480–4. doi: 10.1161/STROKEAHA.114.006297
  157. Okada M, Kikuchi T, Okamura T, Ikoma Y, Tsuji AB, Wakizaka H, et al. *In-vivo* imaging of blood-brain barrier permeability using positron emission tomography with 2-amino-[3-11c]isobutyric acid. *Nucl Med Commun.* (2015) 36:1239–48. doi: 10.1097/MNM.0000000000000385
  158. Jaffer H, Adjei IM, Labhasetwar V. Optical imaging to map blood-brain barrier leakage. *Sci Rep.* (2013) 3:3117. doi: 10.1038/srep03117
  159. Demeestere J, Wouters A, Christensen S, Lemmens R, Lansberg MG. Review of perfusion imaging in acute ischemic stroke: from time to tissue. *Stroke.* (2020) 51:1017–24. doi: 10.1161/STROKEAHA.119.028337

160. Peultier A-C, Redekop WK, Dippel DWJ, Berezki D, Si-Mohamed S, Douek PC, et al. What stroke image do we want? European survey on acute stroke imaging and revascularisation treatment. *Health Pol Technol.* (2019) 8:261–7. doi: 10.1016/j.hlpt.2019.08.005
161. Provost C, Soudant M, Legrand L, Ben Hassen W, Xie Y, Soize S, et al. Magnetic resonance imaging or computed tomography before treatment in acute ischemic stroke. *Stroke.* (2019) 50:659–64. doi: 10.1161/STROKEAHA.118.023882

**Conflict of Interest:** The authors declare that the research was conducted in the absence of any commercial or financial relationships that could be construed as a potential conflict of interest.

**Publisher's Note:** All claims expressed in this article are solely those of the authors and do not necessarily represent those of their affiliated organizations, or those of the publisher, the editors and the reviewers. Any product that may be evaluated in this article, or claim that may be made by its manufacturer, is not guaranteed or endorsed by the publisher.

*Copyright © 2021 Lu, Mei, Hou, Manaenko, Zhou, Liebeskind, Zhang, Li and Hu. This is an open-access article distributed under the terms of the Creative Commons Attribution License (CC BY). The use, distribution or reproduction in other forums is permitted, provided the original author(s) and the copyright owner(s) are credited and that the original publication in this journal is cited, in accordance with accepted academic practice. No use, distribution or reproduction is permitted which does not comply with these terms.*